ACCELERATOR AND INSTRUMENTATION R&D AND CONSTRUCTION

K800 CYCLOTRON STATUS -- MAY 1986

R. Au, S.M. Austin, F.W. Berning, N. Bird, H. Blosser, R. Blue, J. Brandon, B. Brenton, S. Bricker, D. Cole, F. Denovich, J. Dobias, J. Easley, J. Eicher, P. Fighter, R. Fontus, L. Foth, M. Fowler, S. Fowler, R. Fox, L. Gallagher, A. Gavalya, T. Glynn, J. Gonzales, M.M. Gordon, H. Hanawa, Wm. Harder, B. Harper, D. Harris, L. Harwood, S. Hickson, H.P. Hilbert, D. Johnson, T. Jones, B. Jorae, E. Kashy, K. Kranz, H. Laumer, D. Lawton, M.L. Mallory, F. Marti, A. McGilvra, P. Miller, R. Miller, B. Milton, N. Mooney, R. Morin, J. Moskalik, J. Nolen, Jr., Wm. Nurnberger, J. Ottarson, J. Parsons, M. Robertson, D. Scott, C. Scripter, R. Selden, D. Smith, C. Snow, G. Stork, K. Subotic, A. Vander Molen, J. Vincent, R. Welton, R. Zarobinski, and A. Zeller

First beam in the K800 cyclotron is now believed to be less than one year away; internal beam tests are expected to begin in February 1987, and external beam tests should begin approximately six weeks thereafter. At present most major components of the cyclotron are either completed or in an advanced stage of construction (a few components are still in the mechanical design process but on a schedule which will allow them to be released for fabrication, fabricated, and installed in the cyclotron by the end of this year). In general, construction work on the cyclotron is now moving forward at a rapid pace; this in considerable part results from having overcome a significant difficulty which had delayed the project, namely the design of the extraction system. Just at the end of 1985, an extraction system with reasonable field strength requirements and adequate apertures was finally realized in the computer studies; with the extraction design frozen, the yoke of the magnet was quickly modified to include apertures for the various drive mechanisms and beam paths. The modified yoke components were installed in the magnet in late February so that the magnetic effect of these rather large changes was included in the most recent magnet mapping cycle, the primary purpose of this most recent mapping cycle being to verify the magnetic effect of the room temperature trim coil array.

The trim coil mapping is the most extensive of the three magnet mapping cycles which are involved in the cyclotron construction plan. The incremental affect of each trim coil was measured at a variety of main magnet excitations, thereby yielding a data bank which can be used by field fitting codes to determine the trim coil currents required for any desired cyclotron operating point. The required maps were complete as of early May and the magnet has again been disassembled in order to begin installation of rf resonator components and to install the beam pipe and the focusing element drives in the cryostat.

With the magnetic components of the cyclotron coming almost to a state of full completion, the primary effort of the project shifts to the other major cyclotron subsystem, the accelerating system. (The shift in emphasis is clearly noticed in the working areas of the Laboratory by the fact that almost everything which is now being worked on is copper, in contrast with the iron parts which were prominent at earlier stages of the project.) At the beginning of the accelerating system chain, the three large power amplifiers which will supply the radio-frequency power to drive the accelerating structure are now very nearly complete; high power tests of the second and third amplifiers are scheduled to begin in a few weeks, the primary remaining work on the amplifiers consisting of installing control wiring to connect the amplifiers with the rf console at the mezzanine level. Earlier the first of the three amplifiers was extensively tested over its full operating range, with control from a temporary console located

adjacent to the amplifier. In these tests the power output from the amplifier exceeded design requirements by a reasonable margin and the amplifier design is then believed to be firmly established.

The largest rf system components are the "resonators" which consist of the actual accelerating electrode, the "dee", and the dee "stem" which is adjustable in length by means of the "sliding short" in order to tune the structure over the frequency range from 9 Mhz to 27 Mhz, this wide frequency range being needed to cover the very wide deuterium to Uranium operating range envisaged for the cyclotron. Parts for the resonators are being fabricated in our own shops and in outside shops, depending on the special requirements and skills which are needed for particular parts. The resonator structure, for example, involves a number of large copper spinnings which is a fabrication process that the Laboratory is not equiped to handle. Outside vendors, on the other hand, have proved very unreliable in making vacuum tight welds, particularly in copper; a frequently used fabrication pattern for resonator weldments then involves initial rough machining of weldment parts by an outside shop, welding in our shop, and return to the outside shop for finish machining. Defective welds were in particular the cause of one significant set back in the resonator fabrication -- this involved the fabrication of the intricate 86" diameter copper covers which go over the magnet pole tips to provide a high conductivity surface for rf return currents and to isolate the epoxys and other high outgassing components of the trim coil array from the main accelerating system vacuum. Major subelements of these copper covers were ordered from a copper fabricator in Cleveland, Ohio who had submitted a number of leak free samples of copper welds as evidence of qualification. The sample welds were completely adequate -- the welds in the actual parts were on the other hand extremely porous, apparently due to the introduction of some impurity in the fabrication process. The weld impurities hampered repair of the leaks and after a rather large amount of effort, the parts were finally abandoned and entirely new materials were used to proceed with fabrication of replacement components in our own shop. The defective components for the lower hill cover have now been replaced with these vacuum tight, internally fabricated components and the complete lower pole cover is nearing completion. Fortunately, it was possible in this process to rearrange the assembly plan for the cyclotron so that the overall cyclotron schedule could still be maintained in spite of the delay on the pole cap covers.

The two main rf system components which have not yet been released for fabrication are the dees and the sliding shorts. Both of these are at present at the stage of preparation of detailed fabrication drawings. For the dee this primarily consists of a numerically machined aluminum form on which a 3/32" thick copper skin will be placed and formed to the intricate shape by a combination of hammering and welding. The sliding short is somewhat less intricate than the K500 sliding short due to the introduction of a very rugged contact finger which can carry the required rf currents without additional clamping from an array of air cylinders such as is used in the K500 sliding shorts. A prototype of the finger based sliding short has been in operation in the K500 with the finger spacing arranged so that the current per finger in the K500 situation matches that which the fingers will experience in the K800. An initial problem with the prototype short was traced to a poor solder contact between the fingers and the main body of the short. The joint was resoldered using improved fixtures and has thereafter performed satisfactorily.

Smaller K800 subsystems which are still in an incomplete status include the injection system, the extraction system, the vacuum

pumping system and the diagnostic system. Helpfully, the central region of the K800 magnet is arranged so that the K800 injection system can be an exact copy of the injection system for the K500; injection system components will therefore be interchangeable between the two cyclotrons.

The extraction system for the K800 is similar to that for the K500 in that the magnetic elements consist of clusters of small iron bars mounted on motorized position drives which reach through the cryostat. One of the electrostatic deflectors involves a new feature, namely, hinged joints to allow the effective curvature of the deflector to change as needed to match the requirements of the broad range of accelerated ions. A prototype of the hinge detail is being fabricated to check that the design does not impinge on the voltage holding capability of the deflector. The K800 deflector design allows a substantially enlarged insulation space in the feed-through tube where the high voltage lead enters the cyclotron; this is the design detail which is believed to be the present most severe limit on voltage holding capabilities of the K500 deflectors.

The vacuum pumping system for the K800 will be an exact parallel to the system used in the K500, namely a combination of turbo pumps and cryopumps for the accelerating vacuum, and mechanical pumps for the trim coil vacuum. (The main coil cryostat vacuum is pumped down by a mechanical pump/diffusion pump combination and thereafter valved off -- in the most recent operating test of the cryostat the valved off vacuum remained at constant pressure through the full three month testing period -- this is a very desirable characteristic since in the valved off state the insulating vacuum is independent of any electrically powered system and the vacuum will therefore maintain itself in the event of a power failure.)

Possible modifications in the diagnostic systems used in the K800 relative to those used in the K500 are presently under review. The main probe used in the K500 has been especially troublesome and the probe requirements in the K800 are fundamentally more difficult than those in the K500 due to the increased pole tip spiral. Several possible alternate probe designs are being looked at, some of these to the degree of making prototype tests. Hopefully a substantially improved probe system will have been developed by the time we need to freeze the design and begin fabrication.

The remaining work to bring the K800 cyclotron into operation involves two large efforts which are often not considered as part of a cyclotron, namely the hooking up of the hundreds of thousands of utilities and control connections and the development and installation of the control system. Both of these systems will require a great deal of effort from the Laboratory technical staff. Completion of the required tasks on the presently planned schedule does however appear to be compatible with our present staffing level and we therefore do not expect this work to delay the first beam tests.

In summary work on the K800 cyclotron is proceeding at a rapid pace and, since the freezing of the extraction system, work on the project has been basically holding to the planned schedule. It then appears that we will be able to begin beam tests at or close to the presently projected dates.

INITIAL RESULTS WITH A VERTICAL, FULL IRON YOKE, 2 X 6.4 GHZ ECR SOURCE FOR THE NSCL HEAVY ION CYCLOTRONS

T.A. Antaya, Z.Q. Xie

This report describes the design and initial operating characteristics of a new, medium size ECR ion source which is now providing positive ions for injection into the K500 cyclotron. Some features of this source were intended to simplify the mechanical design and thus reduce costs (choosing a vertical orientation, use of the yoke as the support structure, stray field shield and X-ray absorber, and a multi-function plasma chamber). Others were intended to compensate for known difficulties with other designs (an adjustable position first stage, high uniformity hexapole magnet, high symmetry extraction). Others were intended to gauge changes in performance for new ranges of operating parameters: the source has a plasma volume intermediate in size, and for the first time has a minimum B first stage, with both stages operating at 6.4 GHz.

The overall progression of this project is summarized in Table 1. Generally, the project moved quickly, in part aided by the simple mechanical design. An argon plasma was produced July 21, 1985, less than three weeks after the completion of the hexapole. At this point the analysis magnets, actually the first part of the beam transport line to the K500 cyclotron, were not complete, and so it was not until August 31 that analyzed beams were produced. In the fall of 1985 the initial debugging of the new hardware proceeded in parallel with the completion of the beam transport line to the K500 cyclotron. Initially, nitrogen and oxygen ions were tuned; a wide scan of the available parameter space in magnetic field, microwave power and gas flow was performed. This was necessary to reduce the tuning range to begin optimizing the performance. The only serious difficulty during this period was the failure of two quartz microwave feed-through windows in October, which was traced to a localized stress concentration in the vacuum sealing surface of the windows. The clamping non-uniformity was eliminated and the problem did not re-appear.

Table 1. Major Project Milestones.

	1984
July	Order place for microwave transmitters during a design study for a superconducting ECR.
Nov.	Decision to design and built medium size room temperature ECR.
Dec.	Design begins after Hexapole-Octupole conversion test at LBL. Large bore hexapole magnet chosen.
	1985
Feb.	Circular coils wound. Microwave transmitters arrive.
May	Iron return yoke installed over ECR pit area.
June	Hexapole magnet assembled.
July	First plasma.
Aug.	First analyzed beam.
	1986
Mar.	First Injected beam in K500 cyclotron.
Apr.	First nuclear physics experiment.

Two main modes of operation were tuned during this period. The main characteristic of the first mode was that the source optimized with the first stage magnetic field well above that required for an ECR resonance at 6.4 GHz. The ion source did not require the first stage to be on, the first and second stage stage pressures were relatively low when compared to other later modes for this source, and it was

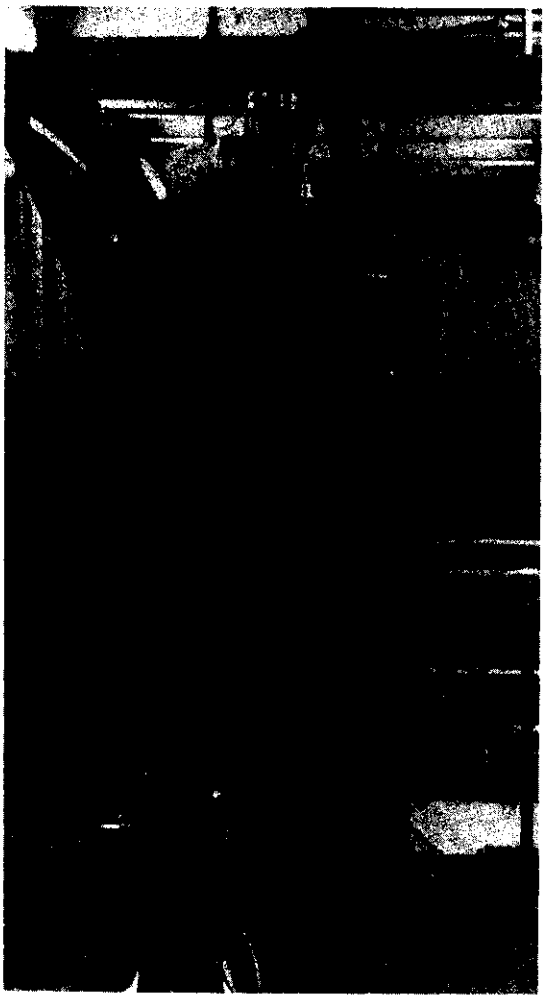

Fig. 1 Photograph of assembled ECR source.

found to be very stable and reproducable. It was possible to find this mode because the coils could be operated well above their nominal currents for a 6.4 GHz first stage. The field profile looks very similar to that of the sources that have a first stage frequency much higher than the second. What is probably happening is that the first stage high field naturally improves the confinement of second stage ions. The best high charge state oxygen results to date for this source have come in this mode.

The second mode had a minimum B zone in both stages -- there appears on the inside of the small first stage chamber a plasma triangle as in the second stage. The magnetic tuning of the minimum B first stage is relatively straightforward. When the first stage field is dropped below a well defined minimum, the output falls off and the percentages of carbon and oxygen ions in the background spectrum increases (copper outgassing). This is interpreted to be due to the ECR zone touching the inside ends of the first stage chamber. In addition, should the first stage be shut off when the field is above a well defined maximum, the first stage will not restart until the field is reduced. Further, the low charge state output of the first stage begins a sharp fall to zero above this maximum, which is found to correspond to the field level at which there is no longer an ECR zone inside the first stage chamber. Thus it has become clear that there is a closed ECR surface inside the first stage for optimum low charge state output. High charge states up to a few nanoamperes of Ar^{8+} have also been observed from this minimum B first stage, though because of its high operating pressure it is still relatively a 1+ ion stage. Substantial tuning of argon ions was performed on this two minimum -B- stage mode during the latter part of Fall 1985.

By early December 1985 argon 8+ peaks in the 75-100 eμA range were achieved. At that point a major development decision was made -- to shift from the study of argon and other light ions to the optimization of the source for heavy mass species. This was done in an effort to look ahead to the ultimate goals of the NSCL facility. Subsequently work began on the production of high charge state krypton ions. A series of studies of the coupling between the minimum B first stage and the second stage, and less importantly other parameters, led to a relatively high pressure, high extracted current, 2 minimum B mode with Kr^{19+} above the 1 eμA level.

With the completion of the beam transport

Table 2. DC ECR Performance.

	^{12}C	^{14}N	^{16}O	^{20}Ne	^{40}Ar	^{86}Kr	^{127}I†
4	25.5	>100	87.	67.	19.		
5	5.6	68.	61.	45.	*		
6	*	13.6	52.	31.4	42.		
7		*	5.1	10.	55.		
8			*	2.3	77.		
9					44.		
10					*	23.	
11					7.0	*	
12					1.0	23.3	
13					0.10†	29.0	1.7
14					0.05†	29.0	2.3
15						23.2	3.0
16						*	*
17						2.6†	2.7
18						1.7†	*
19						1.4†	2.5
20						0.4†	2.3
21							2.1
22							1.8
23							1.0
24							*
25							.035††

Conditions: 10 kV ext. voltage; 8 mm ext. aperature,
† Vertical emittance decreased by 2.0 to increase resolution.
†† Vertical emittance decreased by 6.0 to increase resolution.
* Mixed M/Q

line and spiral inflector in late February 1985, the ion source has become coupled rather heavily with the operation of the K500 cyclotron. During this time it has become clear that the high pressure mode is not optimal for light ions, and the tuning for these has gone in the direction of lower pressures. At the same time a larger first stage chamber has been tried to improve the microwave coupling, the large chamber does indeed improve the operation by making microwave power absorption higher. The disadvantage of going to the larger first stage chamber is that it requires a radial second stage microwave feed, the larger chamber taking

space originally occupied by the axial second stage microwave feed. The successful operation with radial second stage feed required two iterations -- microwave power traveling towards the second stage must in the radial direction pass through an ECR zone on the back side of the hexapole magnet without a plasma forming inside. The initial configuration did allow a plasma in the waveguide, which caused it to be intrinsically unstable. In the second configuration the external ECR zone was crossed at atmospheric pressure by the window inside the radius of the external zone, so that no plasma forms and the radial feed works.

The present overall configuration of the ion source has the larger first stage chamber and radial second stage microwave feed coupled with lower overall operating pressures in the two stages. The initial trials of this geometry have led to significant increases in high charge state neon and nitrogen ions over previous levels, and there is an expectation that this can be extended to other species when the cyclotron schedule permits further development.

BEAM TRANSPORT LINE FROM THE ECR ION SOURCE TO THE K800 CYCLOTRON

S. Tanaka, J.A. Nolen, and A.F. Zeller

Ths ECR ion source which is now working coupled with the K500 cyclotron is supposed to also provide beams to the K800 cyclotron. In designing the beam line to the K500 cyclotron, the possibility of directing the beam to the K800 cyclotron was taken into account. The 90° analyzing magnet was made rotatable around the vertical beam axis, so that it can send the beam in other directions in the horizontal plane. The new beam line to the K800 cyclotron starts from the analyzing aperture located after the 90° magnet.

The design of this beam line has been accomplished with four solenoids and four bending magnets. These elements are almost the same as those used in the existing beam line to the K500 cyclotron. This will save us design time. Fig. 1 shows the layout of the beam line. The beam comes straight down from the bottom of the ECR and is bent by 90°. All magnets are sitting in a horizontal plane. The last 90° bending magnet is located just below the center of the K800 cyclotron and bends the horizontal beam to the upward direction. Fig. 2 shows the envelopes of the beam in both x-z and y-z planes, as calculated with the TRANSPORT program. The beam which is stigmatic at the

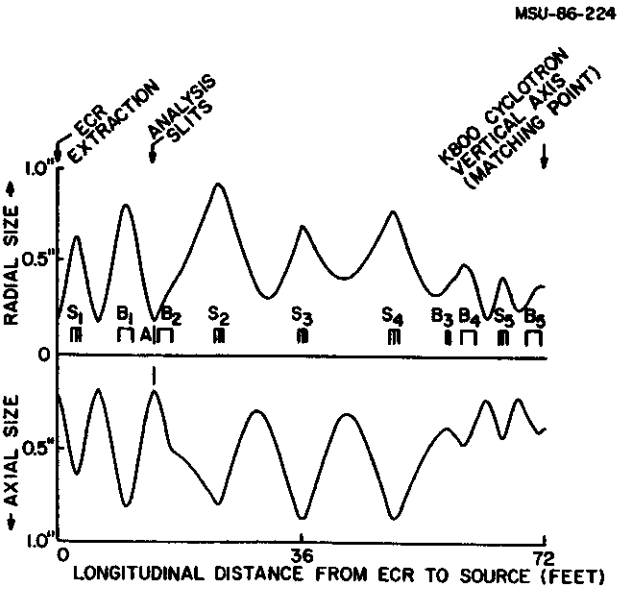

Fig. 2 The envelopes of the beam in the X-Z plane (the upper half of the figure) and in the Y-Z plane (the lower half of the figure). The initial beam profile of 5mm x 20mrad turns into a waist of 10mm x 10mrad at the end of the beam line.

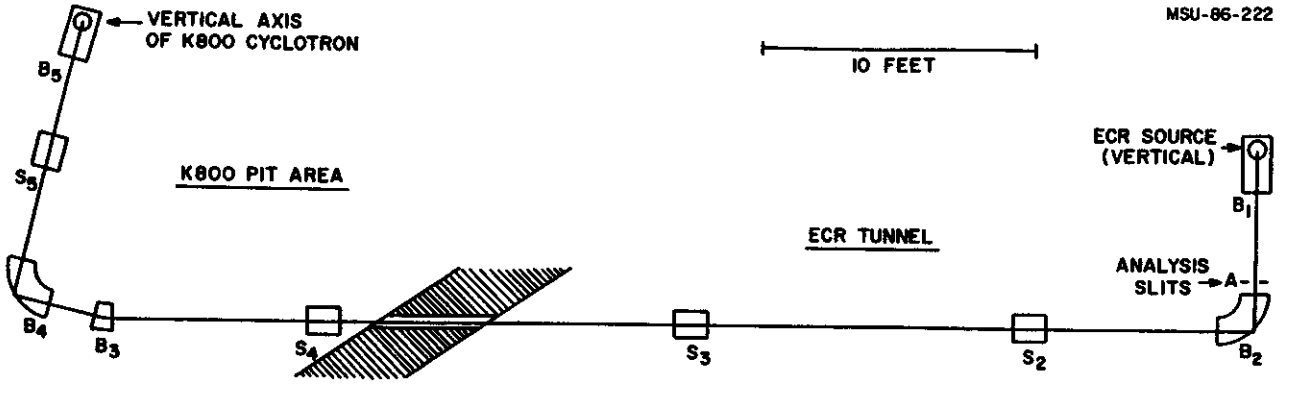

Fig. 1 The layout of the beam line. B denotes bending magnets, S the solenoids and A the apertures. The first solenoid S1 is not shown in the figure.

analyzing slit indicated by A gets astigmatic after passing through the next 90° bending magnet B_2, because of space limitation in the beam line pit. For the beam transmission to the third bending magnet, to keep the beam size smaller than 1 inch, three solenoids are used. After each solenoid, the beam forms a waist where 4-jaw slits will be installed for beam diagnosis. At this point, the beam magnification is approximately 2. A set of three bending magnets and one solenoid leads the beam from the tunnel to the bottom of the K800 cyclotron. And also this part of the beam line makes the beam stigmatic again at the K800 vertical axis. The final beam profile matches the acceptance (±10mm X 10mrad) of the axial injection beam line.

THE ECR TO K500 AXIAL LINE OPTICAL DESIGN

A.F. Zeller, J.A. Nolen Jr., and L.H. Harwood

The preliminary optical design by Harwood,[1] presented in last year's annual report, for transport of ECR beams to the K500 axial line has been finalized and the line constructed. The final design used the solenoid option, instead of quadrupoles. Generally solenoids require more power than quadrupoles, but at these very low rigidities this disadvantage is offset by the advantages of solenoids: viz. 1) smaller beam envelopes, 2) half as many magnetic elements, 3) very simple beamline tuning, and 4) nearly symmetric x and y beam envelopes.

The assumed emittance was (5mm x 20mr)π in both planes. Although the physical sizes of the dipoles [2] and solenoids [3] accept divergences of up to ±40 mr, second order effects (mainly x/θ^2 and x/ϕ^2) result in encreased spot size at the analysis Faraday cup for such large divergences. The system was also designed to transport a maximum beam rigidity of 34MeV/c, but the maximum Bρ accepted by the spiral inflector - K500 Cyclotron System is 12.4 MeV/c. Hence, for ECR studies the 90° analysis magnet and first solenoid are wired and cooled to permit use at the maximum rigidity (34 MeV/c), while the remaining elements are only wired and cooled to tranport the lower rigidity (12.4 MeV/c).

The required beam shape at the beginning of

Table 1:

Summary of ECR Analysis System and Tranport to K500 Axial Line.

Assumed ECR output beam:	±5mm x ±20mr, x and y
Momentum for this case:	10 MeV/c
Drift from extraction electrode to solenoid 1:	2.5'
Solenoid 1:	1.24' long, B=1.63 kG, I=74 A
Drift to object slits:	2.5', unit magnification
Drift to divergence slits:	2.5'
Drift to 90° magnet:	0.6'
90° magnet:	ρ=1.33', B=0.82 kG, I=78 A, y-focussing edge angles = 30.7°
Drift to image (analysis) slits:	3.1', unit magnification
Drift to solenoid 2:	4.4'
Solenoid 2:	1.24' long, B=1.28 kG, I=58 A
Drift to waist:	4.4', unit magnification
Drift to solenoid 3:	4.4'
Solenoid 3:	same as solenoid 2
Drift to waist (through K500 wall):	4.4', unit magnification
Drift to 23° magnet:	0.75'
23° magnet:	ρ=2.67', B=0.41 kG, I=39 A, y-focussing edge angles=7.2°
Drift to solenoid 4:	1.0'
Solenoid 4:	B=1.44 kG, I=65 A
Drift to 90° magnet:	4.35'
90° Magnet:	same as first 90° magnet
Drift to waist (matching point for axial injection):	0.92', magnification=2

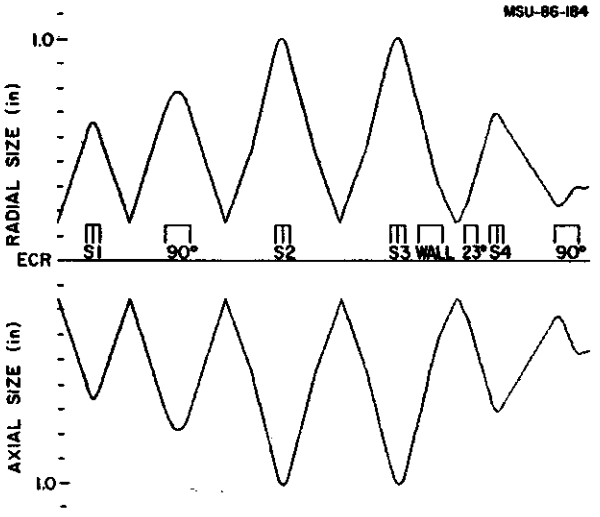

Fig. 1 Beam envelopes in both planes from the ECR to the axial line. For scale, the wall is 2 feet thick. Devices labled S are solenoids, while dipoles are labelled with the bend angle. Note that the 23° dipole bends in the horizontal plane, while the 90° dipoles bend in the vertical.

the axial line[4] for maximum transmission is ±10 mm x ± 10mr in both planes. The beam envelopes from the ECR to this point are shown in Figure 1. The horizontal axis can be scaled from the width of the wall (2 feet thick). Waist-to-waist focusing was used throughout. Table 1 gives a more complete description of the line. Operational experience shows that the required currents in the magnetic devices are predicted by the calculation with ~1% accuracy.

References

1. L.H. Harwood, MSU Ann.Report 1983-84, p276
2. A.F. Zeller, J.A. Nolen Jr., and R.T. Swanson, this Report
3. ibid.
4. F. Marti, ibid.

ECR BEAMLINE DIPOLE MAGNETS

A.F. Zeller, J.A. Nolen, and R.T. Swanson

Three dipole magnets have been constructed and installed in the ECR to K500 beamline, one which gives a 23° bend and two with 90° bends. The design of the 90° magnet has been presented previously[1], while the 23° magnet is just a shorter version of the 90° design. The only design change from that presented last year was to increase the gap from 4.17" to 4.24" to better accomodate the coil package. This increased the current required to reach 2.5 kG to 238A, since the magnet produces 10.5 G/A in its present configuration.

To facilitate coil winding, the coils did not parallel the ends of the magnet, but were bent thru two 90° angles to clear the beam space. This resulted in the end coils being perpendicular to the beam axis instead of at a 30° angle to it. This is shown in figure 1. The net result is that the coil extends further in the beam direction at larger radius, hence giving a smaller edge angle than dictated by the iron. Since this angle produces the y-focussing necessary to produce a double image, it must be adjusted by using an iron shim on each end of the magnet. The effect of the shim is to short circuit the excess field created by the extended coil. Varying the length and position of the shim produces the correct angle by successive mappings. Some curvature of the effective edge may result from the shimming but our field maps indicate that this is a small effect. Figure 1 shows the location of one of these shims. Empirical measurements of the x and y image locations will be made during 1986, to verify

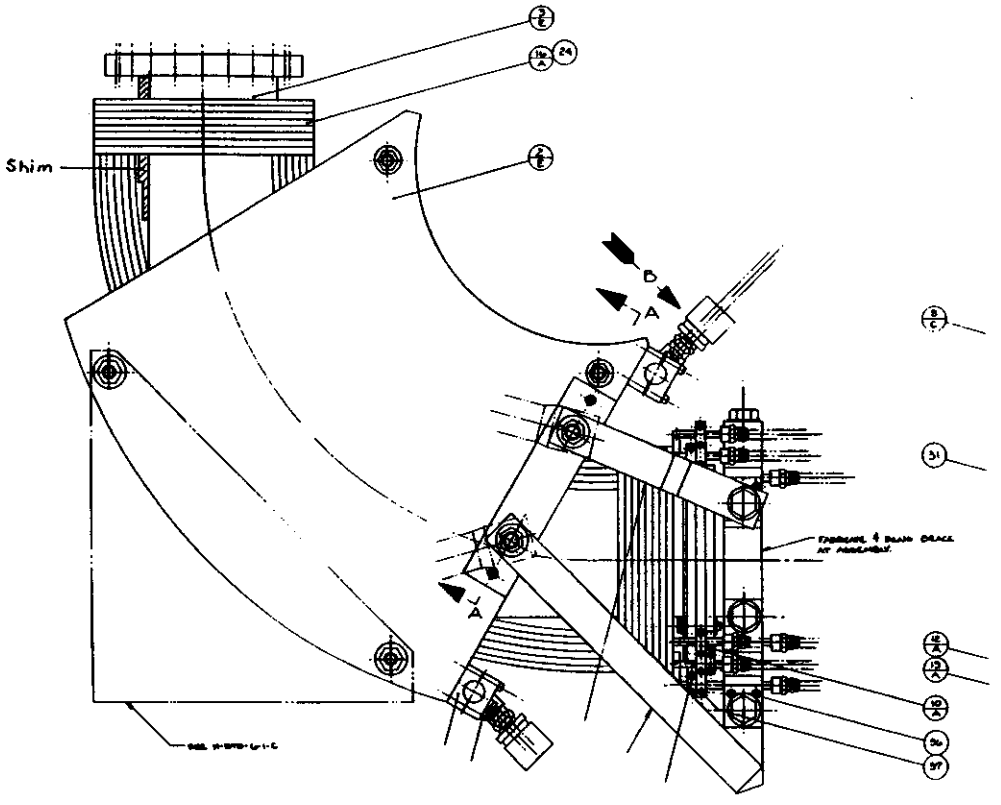

Fig. 1 The 90° dipole magnet, showing the yoke and coil. One of the shims is also shown.

that the present shimming is correct or to generate data for fine tuning of the shimming.

The effective length is also changed by the shimming procedure. Since the angle can change from 17° (unshimmed) to over 45° (completely shorted) by pivoting about the unshimmed side, the effective length clearly changes. After shimming, the effective field boundary extends 2.48" outside of the physical edge (1.17 half-gaps). The length is relatively constant with excitation, changing only 0.16 mils per amp, or 0.04" at 250 A. An installed 90° magnet is shown in Figure 2.

Fig. 2 The analysis 90° dipole in place under the ECR.

The 23° dipole is basically rectangular instead of wedge-shaped. Coil sizes, gaps and pole width are the same as the 90° magnets. To get the maximum use of the volume of good field, the beam enters and exits a rectangular magnet at an 11.5° angle. This provides no x-focussing. In order to preserve the approximate symmetry of the x and y phase space, some of this x-focussing was restored by providing small edge angles. Figure 3 shows the details of the 23° magnet. Note that the magnet also has extended coils like the 90° dipole. However, no shim was used since the measured angle, 8.7°±.7°, was close to the expected value of 7.2°. Additionally the optics are not very sensitive to this angle. Figure 4 shows the magnet in place in the K500 vault.

The 23° magnet is designed to run at half the 90° current, since it has twice the radius of curvature, and still provides 10.6 G/A up to

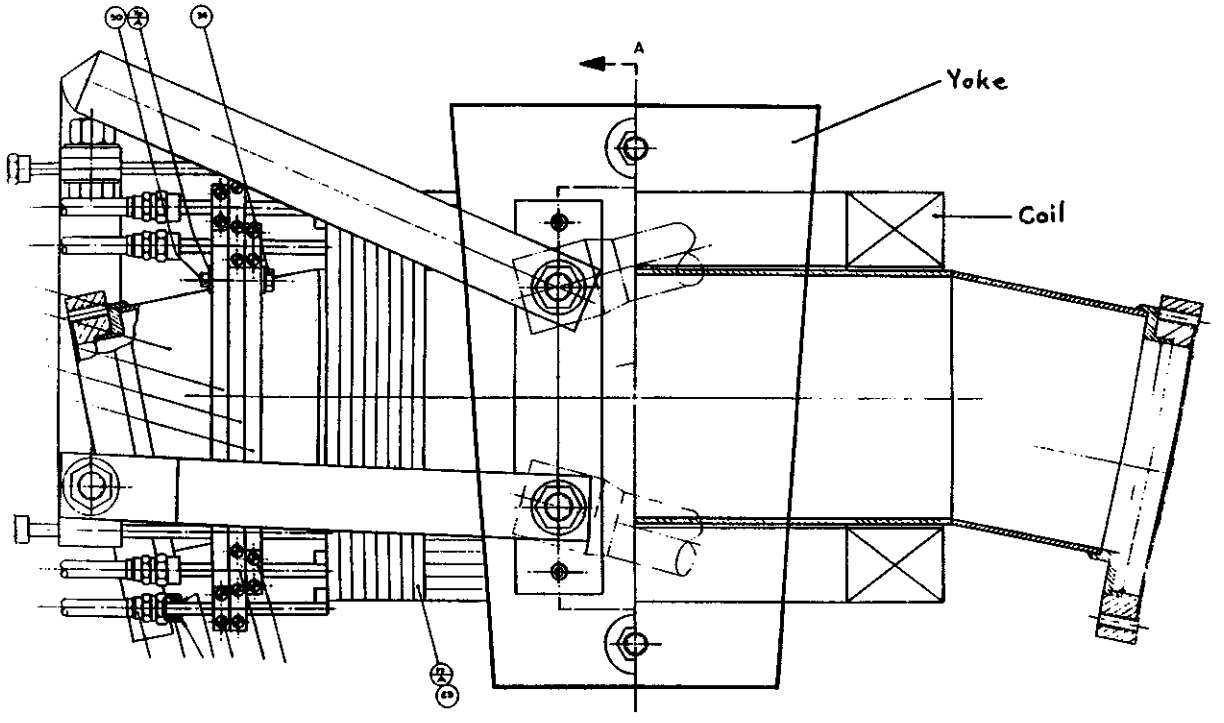

Fig. 3 A top view of the 23° dipole assembly.

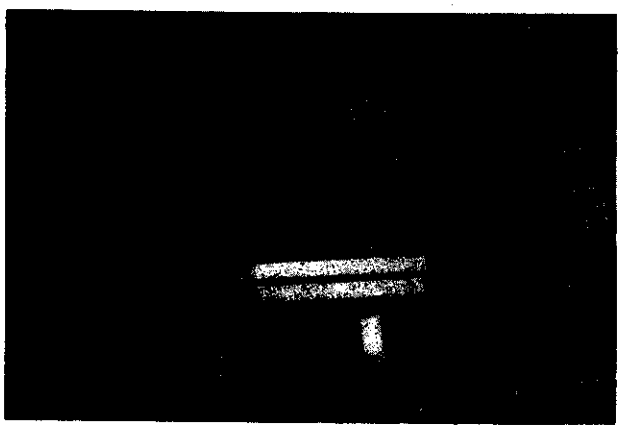

Fig. 4 The 23° magnet in place in the K500 vault. This is a view looking up at the magnet.

a maximum of 1.25 kG.

All of the magnets have performed satisfactorily, although as mentioned above we will test to see if the 90° magnet actually produces a double focus at the analysis slits, as designed, or if corrections are necessary.

References

1. A.F. Zeller, J.A. Nolen, and R.T. Swanson, MSU Ann. Rep. 1983-84, 279.

ECR BEAMLINE SOLENOIDS

A.F. Zeller, J.A. Nolen, and R.T. Swanson

The ECR to K500 axial beamline requires the use of four of the 6" diameter solenoids, described in last years annual report.[1] Additionally, the axial injection line requires another solenoid, having a smaller outside diameter necessary to fit between the dee stems.

The iron yoked solenoids, used under the ECR source, and along the horizontal section of the beamline produce 22 G/A, and have effective lengths also in excellent agreement with the POISSON calculations. One of them is shown installed in the beamline in figure 1.

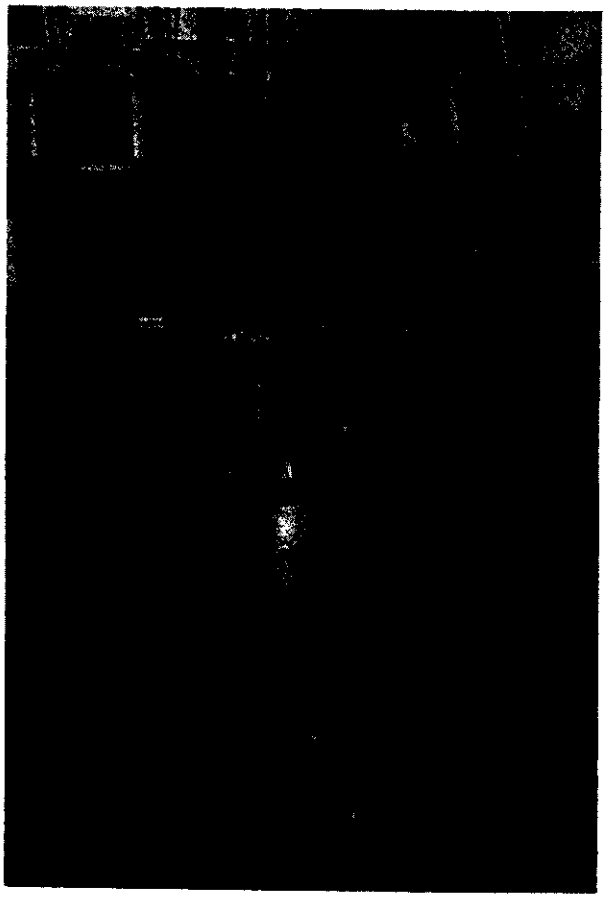

Fig. 1 Standard iron yoked solenoid installed in the ECR beamline. The copper pipes around either end are the entrance and return water manifolds.

The other type of solenoid for use under the cyclotron is a "naked solenoid", ie, a standard air core solenoid without an iron return yoke. An iron yoke could not be used because the axial injection optics uses the solenoidal field of the K500 for focussing, while the naked solenoid is used to trim the field. The lack of a return yoke is not serious since the central field is only decreased by about 10%. The parameters of the naked solenoid are listed in Table 1. Shown in figure 2 is the solenoid before installation between the dee stems.

Table 1

Naked Solenoid Parameters

Length (effective and physcal)	13.5"
Inside diameter of coil	6.0"
No. of turns of 1/4" wire per layer	50
No. of layers	10
Current (2.0 kG)	133 A
Power (2.0 kG)	3.5 kW
Water flow @ 80 psi	1.1 gal/min
Max. Temp rise	17°C

Fig. 2 The naked solenoid prior to installation. Two successive layers are connected in series hydraulically. The pipes are the water manifolds.

Five more iron-yoked and one more naked solenoid will be built for the ECR to K800 beamline.

References

1. A.F. Zeller and J.A. Nolen, MSU Ann. Report 1983-84, 281.

ECR BEAMLINE X-Y STEERING MAGNETS

M.F. Williams, A.F. Zeller, and J.A. Nolen

Steering Magnet Requirements

The steering magnets described in this report were required for the ECR beam-line in five places to provide corrective steering capabilities. Four magnets were wound on steel cores and produce ~100 gauss at five amps, and the fifth was wound with an aluminum core and produces five gauss at five amps. The most noteable magnet is the aluminum cored unit which is mounted above the last 90 degree bending magnet and directly below the K500 cyclotron. This magnet serves as a fine tuning device after the 90 degree magnet bends the beam upward into the K500 axial line. All of these magnets are air cooled.

Three magnets were designed with leg-type supports and mounted on the floor along the ECR beamline, and the remaining two were designed to lay face up on posts that attach to bellows' bolt circles.

Magnet Design and Components

Each steering magnet, shown in figure 1, consists of four identical flat coils, each with 430 turns of 14 AWG wire, bolted together at the ends to form a square 8" x 8" inside. This design allowed easy installation because only one side needed to be removed to be able to slip the rest of the magnet over the beam pipe.

The steel cores (1020) of each coil, 1" x 5" x 9.5", were first machined to length, then drilled and tapped. The faces were then insulated with .010" G-10, and wooden spacers and half-rounds epoxied on. Finally, a removeable handle was bolted on one end to hold the unit for winding. The winding was performed on a lathe, with a simple nylon tensioning block

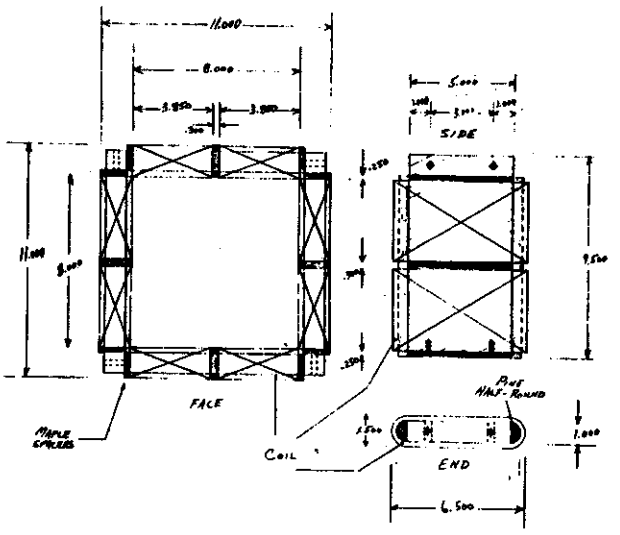

Fig. 1 Three-view mechanical drawing showing face, side and end of side. The maple spacers and pine half-rounds are shaded. The coils are designated with an X.

mounted in the tool holder, by drawing the wire from a spool positioned on a nearby table.

Two coils are in series for each of the X and Y directions. (Electrical schematics of these magnets and their power supplies are shown in a separate progress report.) The steel within the coils parallel to each other in the horizontal become the poles for the vertical coils when powered and vice-versa.

The wooden spacer in the center of each coil produces a gap in the coil which creates a more uniform calculated field at the center of the magnet, compensating for the gaps that must occur at the ends of each coil to allow clearance for assembly.

Field Data: Steel-Core Unit

Two coils in series, totaling 860 turns of

14 AWG copper wire have a resistance of ~2.6 ohms. At five amps, the maximum field observed at the center of the magnet was 102 gauss. Therefore B(I) = 20 gauss/amp, V(5A) = 13.0V, and P(5A) = 65W.

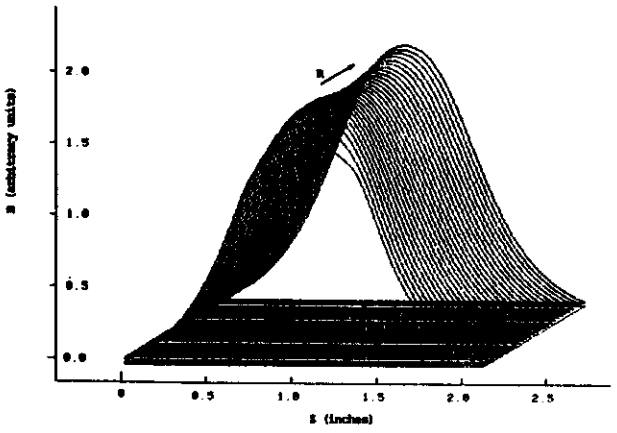

Fig. 2 Field strength B distribution pattern generated from mapper data. R axis is across the face of the magnet and each run through the magnets' Z axis was separated by 1/5 inch.

Figure 2 shows the field strength distribution of the magnet with respect to Z through the magnet perpendicular to the face, and R across the face in the median plane. Mapping was performed with the NSCL mapper which runs a small rigidly supported coil of fine wire through the magnets' Z axis. Each run through the magnet was separated on the R axis by increments of 1/5 inch.

Figure 3 shows the 2-dimensional POISSON calculation of the normal field compared with the measured fields showing the slight asymmetry between left and right and the X and Y fields. The asymmetries are primarily due to the inhomogeneous gaps that naturally occur at the corner interface of any two coils because of irregularities in the metal surfaces, machining tolerance errors, and non-uniform torques on the bolts. The large deviations of the measured fields from the calculated fields are basically the result of applying a 2-dimensional code to a problem which is really 3-dimensional. Because the length (the effective length is 10") is

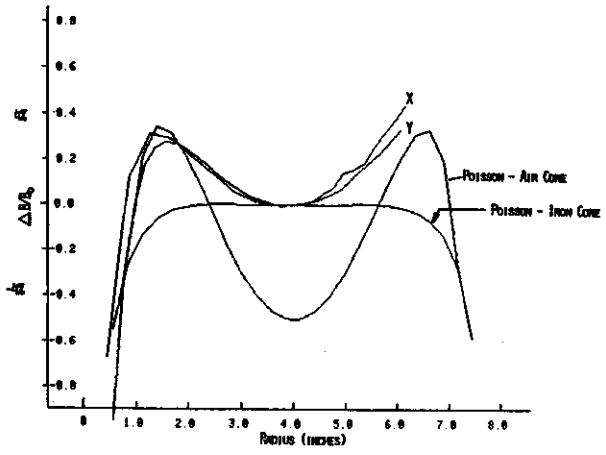

Fig. 3 Two-dimensional POISSON uniformity calculations for the air core and the iron-yoked cases. The measured X and Y fields of the iron-yoked magnet are also shown. The ordinate is the deviation from the central field in percent. Note the asymmetry between X and Y.

short with respect to the transverse dimensions, the problem is not adequately simulated by POISSON. POISSON, for example, predicts central fields for the iron and air core cases of 12G and 17G, respectively, while the measured fields are significantly lower. Qualitatively, we believe that the central field is depressed relative to the 2-dimensional calculations due to the finite-length effect. The field increases a few percent as one moves from the magnet center towards the coils on either side because the finite-length effect is reduced enar the coils. We are planning a second-generation of these steering magnets for the ECR-K800 injection beam line, and hope to improve the field uniformity for changing the coil design to compensate for the finite-length phenomenon. Figure 4 shows the POISSON calculated field lines produced with both the X and Y coils powered equally. The sum of the two fields produce nearly perfect 45 degree fields lines.

It was required that one magnet be positioned on the beamline near an iron shielding tube in the K500 vault. Figure 5 shows the field clamping effect of the iron tube with respect to the normal field produced with

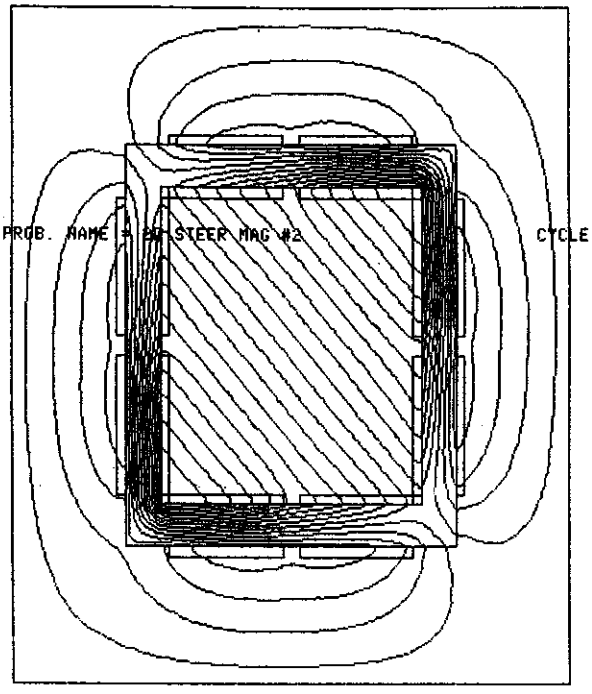

Fig. 4 POISSON calculated field lines produced with both X and Y coils powered simultaneously. With no asymmetry between the X and Y fields the lines would make perfect 45 degree angles.

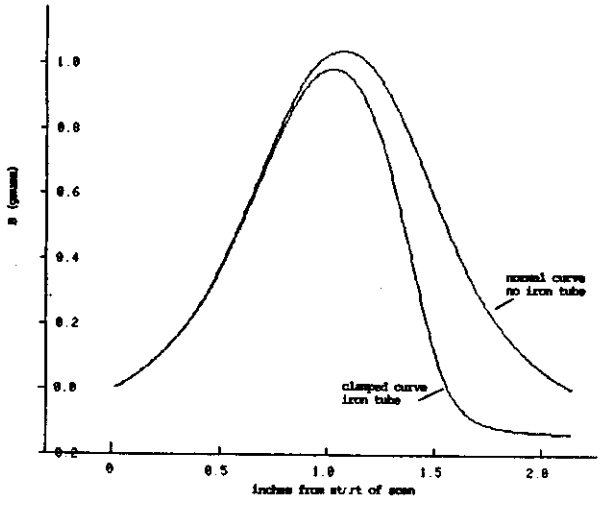

Fig. 5 Field clamping effect produced when an iron shielding tube is placed next to the magnets' face on the Z axis. Also shown is the normal field curve with the tube removed.

the tube removed. The area between the normal curve and the clamped curve is proportional to the mu and mass of the tube and its relative position with respect to the magnet.

Figure 6 shows one of the floor mounted magnets in position on the ECR beam-line.

Field Data: Air-Core Unit

The air- or aluminum-core unit is very weak, producing a central field of 5G at 5A. The z-dimensional calculated field uniformity is displayed with the steel-core magnet data in figure 3.

Fig. 6 One of three floor mounted models installed on the ECR beam-line.

Magnet Costs

About 14 man-hours were required to build each magnet including assembly. At $0.60 per pound, steel costs for each magnet were about $30.00. The copper wire at $0.10 per foot cost about $180.00 per magnet.

MULTIPLE-OUTPUT DC POWER SUPPLY FOR STEERING MAGNETS ON THE ECR ION SOURCE BEAM LINE

S. Tanaka, J.A. Nolen, and Y.R. Lan

Misalignment of magnets and magnetic fringing fields in the beam line from the ECR ion source cause shifts of the beam at the image points. For the purpose of correction of these shifts, steering magnets are installed near each focussing magnet. They make many small DC power supplies of the same type necessary. The features required for the power supplies are (1) they should be current-stabilized, (2) the output current should be bipolar, (3) the maximum current is 5 amp. For steering magnet power suplies it is important that they be able to operate near zero current with either output polarity, ie. with no discontinuities as the output polarity is tuned through zero.

A multi-output DC power supply has been designed to fulfill these functions. Fig. 1 shows the block diagram of the circuit. Two DC power supplies which have an output capacity of 50 A supply $+V_s$ and $-V_s$ to APEX PA12A power operational amplifiers. Each amplifier feeds a current to a pair of coils in the steering magnet. The -IN terminal on the amplifier can accept the output-control signal from a computer. The output current can be monitored by the computer with a shunt resistor which is inserted serially in the output loop. All amplifiers are packed compactly in a NIM-size bin.

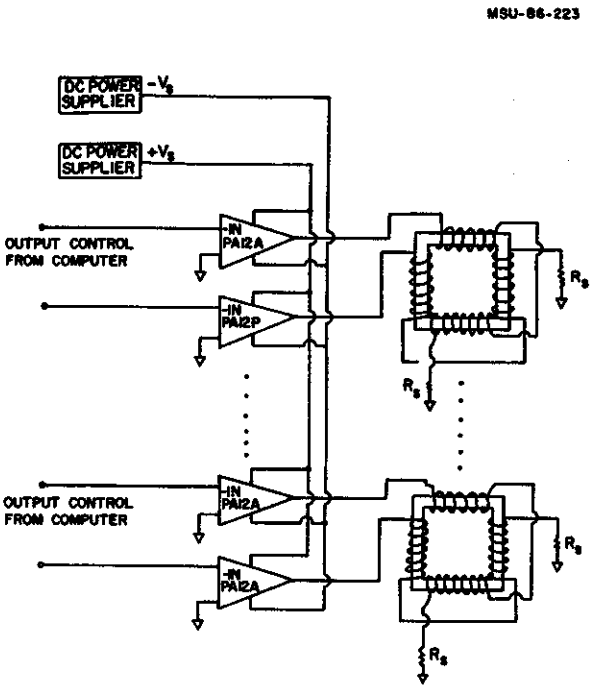

Fig. 1 The block diagram of the DC power supply for steering magnets.

A unit with ten outputs of ±5 amps at ±15 volts has been constructed and is in use on the ECR-k500 beam line.

CONSTRUCTION AND TESTING OF THE PROTOTYPE SUPERCONDUCTING BEAMLINE QUADRUPOLE

A.F. Zeller, R.T. Swanson, J.A. Nolen Jr, J.C. DeKamp

The prototype superconducting beamline quadrupole has been completed and sucessfully tested. Additionally, a dummy quad was used to test the cryogenic aspects and the batch-filled mode for cryogenic operation of the beamline magnets. Preliminary results have been published elswhere.[1]

The magnet went beyond the maximum required current of 13.3A to 14.3A without the need for any training. Measured fields indicate that gradients greater than the design goal of 7.3 kG/in were achieved. The field increase was linear with current until about 12A, corresponding to a gradient of 6.6 kG/in, in agreement with the POISSON calculations. The effective field boundary was measured to extend 3.8 cm beyond the physical edge of the iron. This corresponds to an effective length of 43.1±.4 cm at a low gradient of 2.7 kG/in. At 5.4 kG/in the length is 43.6±.4 cm, i.e. it is constant within the uncertainty of the measurements. The change in gradient along the beam axis was also measured to allow extraction of fringe field coefficients for use in ray tracing. The measured shape of the fringe field is not significantly different from the one previously used in ray tracing.

The magnet was mapped with the apparatus built for the K800 cyclotron mapping but with a coil system[2] which uses two small coils to cancel the signal induced in a large coil by the dipole and quadrupole components of the field. This leaves only the error components for harmonic analysis since it removes contributions from misalignment of the mapping arm and the much larger quadrupole field. It also eliminates spurious signals from speed variations and vibrations. Figure 1 shows the signal from the large coil (direct) and the summed signal (bucked) from a typical map. Note

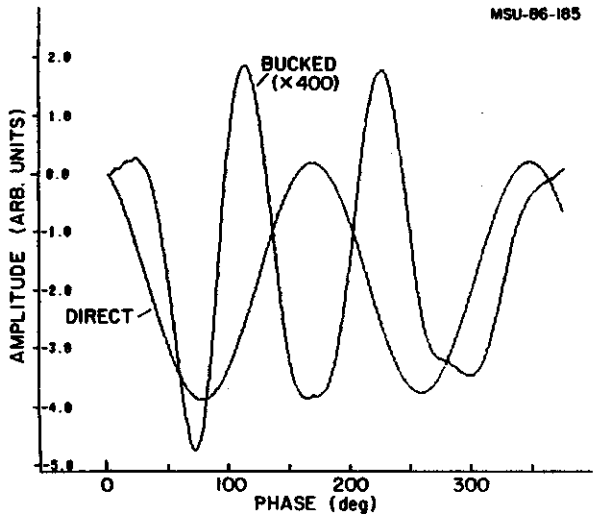

Fig. 1 Output of the mapper for the single (direct) coil showing the phase and amplitude of the field, integrated from zero to 1.85" radius. The bucked signal for the same field level, multiply by 400.

the large reduction in the absolute amplitude of the bucked signal. In practise, not all of the quadrupole and dipole components are removed, but the residual sextupole component is clearly visible.

It is well known[3] that multifilamentary superconducting wire is subject to induced residual fields which depend on the magnetic history of the conductor. Unfortunately, the residual field is rich in higher order multipole components, which may be expected to influence the uniformity of the field at low gradients, especially after high current operation. Figure 2 shows the mapped fields at zero current (bucked). The curve labeled "cold" was taken the day after the peak field run and the "warm" was taken after the magnet was warmed to room temperature. The warm map represents the induced magnetization of the pole tips, since the superconducting magnetization disappears at the transition temperature, and gives the

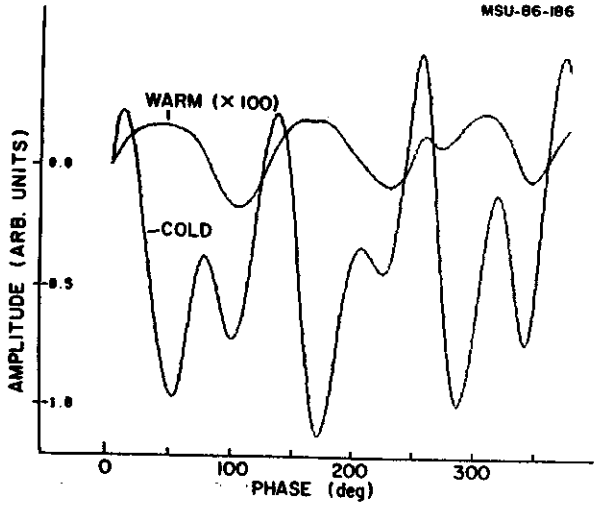

Fig. 2 Bucked signals at zero current for the quad while superconducting and after it was warmed to room temperature.

construction error. The absolute magnitude of the field at the pole tips is only 3 gauss. The magnitude of the coefficients, relative to the quad field are given in tables 1 and 2 for a radius of 1.5". The calculated allowed field errors are given in Table 1, while the measured harmonics are listed in table 2 for several field levels. The magnitudes and the relative ratios of the non-allowed terms, eg. the sextupole and octupole components, indicate[4] that one of the pole tips is either dimensionally inaccurate or slightly out of position, or both.

Cryogenic tests were performed over long periods, necessary for such small boil-off rates. The initial results for liquid helium consumption for both the dummy and the real quad

Table 1

Calculated harmonic coefficients at a 1.5" radius and 6 kG/in.

N	B_N/B_{quad} ($X10^{-3}$)
6	0.25
10	0.01
sum of higher allowed	0.11

Table 2

Measured harmonic coeffiecints normalize to 1.5" radius in units of $B_n/B_{quad} \times 10^{-3}$.

	Gradient (kG/in)				
N	0(warm)	0(cold)	2	6	7.3
3	1.29	1.80	1.79	1.75	1.58
4	0.38	0.30	1.25	1.21	1.21
5	0.13	0.18	0.32	0.36	0.42
6	0.39	1.93	0.53	0.52	0.60
7	0.09	0.30	0.05	0.06	0.06
8	0.05	0.14	0.04	0.04	0.04
9	0.04	0.02	0.03	0.03	0.04
10	0.08	0.17	0.03	0.04	0.05

were disappointing. The dummy used about twice the calculated amount while the real quad used about four times. Liquid nitrogen use was good on both devices. It was then discovered that we had a major problem with thermal-acoustic oscillations in the helium feed lines. (Discussion with R. Powers helped us to identify this problem.) Allowing a small amount of gas to flow thru the lines reduced the loss to a tolerable level. The required usage of less than 25 l/week for both liquid nitrogen and helium was met. The results are summarized in Table 3.

The prototype has been proven satisfactory. We are therefore, proceeding with procurement/construction of the remaining (~60) quads needed for phase II running.

Table 3

Cryogenic results for the prototype quad. Liquid helium usage at 1.2 atmosphere (pump suction).

Cryogen	design (l/hr)	measured(l/hr)
nitrogen	0.102	0.143
helium	0.109	0.133

References

1. A.F. Zeller et al, Proc. Ninth Int. Conf. Magnet Tech, 160 (1985).
2. R.M. Main, J.T. Tanaka and K. Halbach, IEEE Trans. Nucl. Sci, NS-26, 4030 (1979).
3. M.A. Green, IEEE Trans. Nucl. Sci NS-18, 664 (1971).
4. J. Cobb and R. Cole, Proc. Int. Symp. Magnet Tech, 431 (1965).

BEAMLINE DIPOLE PROGRESS REPORT

J.C. DeKamp, C.T. Magsig, J.A. Nolen, A.F. Zeller

The ±16° superconducting switching magnet, whose initial design and testing was described in earlier reports[1-5], is presently at it's midpoint of construction. Many mechanical design changes have occured in the past year to eliminate construction problems and provide operational reliability. This has also slowed construction. Major design changes have occurred in the coil bobbin, current lead assembly, and LHe feed and cold gas return lines.

A new bobbin weldment was designed and built because of leak and distortion problems in the original bobbin. The design cut the total length of weld by over 50%, and eliminated these problems. The coils were packaged into the bobbin using aluminum channel, "Scotchply" tape, and G-10 with the "Scotchply" tape cured after the coils were completely packaged in the bobbin. This assembly is shown in Fig. 1. The bobbin covers were then welded in place with no damage to the coils being found. The completed bobbin/coil assembly is shown in Fig. 2.

The current leads were redesigned from disconnectable, conduction cooled to disconnectable, vapor cooled to eliminate problems with cold feedthru reliability. The new design also has the advantages of attaining faster thermal equilibrium when connected, lower heat transfer while connected giving the option of leaving them connected for extended time periods, and are designed so the entire lead and persistent switch assembly can be installed or removed for repair as one unit with a minimum of trouble.

The LHe feed and cold gas return lines were redesigned based on results of Prototype Quadrupole testing[6] which showed that thermal acoustic occillations were present in the small diameter coiled lines. The small diameter

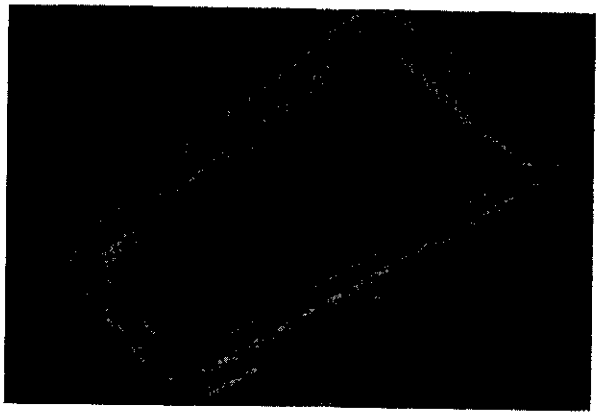

Figure 1.

Figure 2.

coiled line was still needed for it's flexibility so the solution was to eliminate the temperature gradient in this portion of the line. This was done by intercepting the valve at one end and placing a high resistance intercept at the other end. The valve is intercepted in such a place so as the heat transfered to the LHe during filling is actually reduced. The high resistance intercept adds some heat during filling, but together with the valve intercept approximates an unintercepted valve filling condition. The coiled flexible

Figure 3.

line is then thermally isolated during operation by a larger diameter, thin walled tube which should not have occillation tendencies.

Other progress includes completed LNz and LHe containers with thermal shielding partially assembled (Fig. 3), waiting for completion of

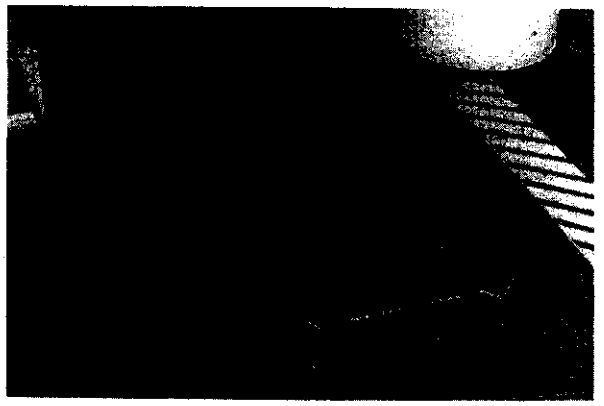

Figure 4.

Figure 5.

the new feed and return line assemblies. The bobbin cryostat wall is partially welded (Fig. 4) and the pole tips have been fit to the yoke with proper spacers welded in place to maintain spacing. The yoke and ple tips are shown in Fig. 5 with the uper yoke slab removed. It is projected that testing will begin this summer.

References

1. A.F. Zeller et al, MSU Annual Report 1981-1982, 101.
2. M.J. Dubois, A.F. Zeller, and J.A. Nolen, MSU Annual Report 1982-1983, 155.
3. A.F. Zeller et al, ibed, 151
4. J.C. DeKamp et al, IEEE Trans. on Mag. Mag 21, 990 (1985).
5. J.C. DeKamp et al, MSU Annual Report 1983-1984, 266.
6. J.C. DeKamp et al, MSU Annual Report 1984-1985.

REMOVING ROOM TEMPERATURE SHORTS FROM POTTED SUPERCONDUCTING COILS

A.F. Zeller, J.C. Dekamp, and J.A. Nolen,Jr.

A persistent problem in winding potted superconducting coils, which have only a varnish for electrical insulation, is a room temperature short. While most shorts are not observed when the coil is cold, their presence may be manifested in the inability to perform magnetic field mapping at room temperature of a device employing such coils. Since correcting possible coil positioning errors is much easier to do before the magnet is welded shut and cooled down, a short which prevents room temperature mapping can be costly in terms of disassembly time or wastage caused by having to wind all the coils without any having shorts. We have discovered a simple remedy for removing these room temperature shorts which works for our small, many-turned potted coils.

We are constructing a prototype superconducting quadrupole for use in the beam transport system at the National Superconducting Cyclotron Lab. The quadrupole uses four identical coils, each of which consists of 3600 turns of 0.3 mm diameter NbTi wire. The electrical insulation is provided by a single build (nominally 0.025 mm) of formvar. The 3.62 km of wire are wet wound with STYCAST 2850FT epoxy with Catalyst 11 (Emerson and Cuming, Inc.) in a nonstructured method (random wound). The coils are cured for 2 hours at 100° C, then post cured for 4 hours at 150° C. One of these coils is shown in figure 1 and a cross section thru the coil in figure 2. Unfortunately, of the 8 coils wound, 4 had significantly lower resistances or inductances (measured at 1 kHz), indicating shorts. The average resistance and inductance of the non-shorted coils are 960Ω and 6.60 H, respectively. The variation in inductance is ±2%. Five of these coils, four without and one with shorts, were tested at 4.2 K to observe their superconducting characteristics. All coils, including the shorted one, ran at the calculated critical current produced by their self fields, reaching that current with at most two quenches. The external magnetic fields levels were found to be identical.

During installation in the quad, one of the non-shorted coils was damaged, necessitating the use of the shorted coil which had been previously tested. Upon testing after

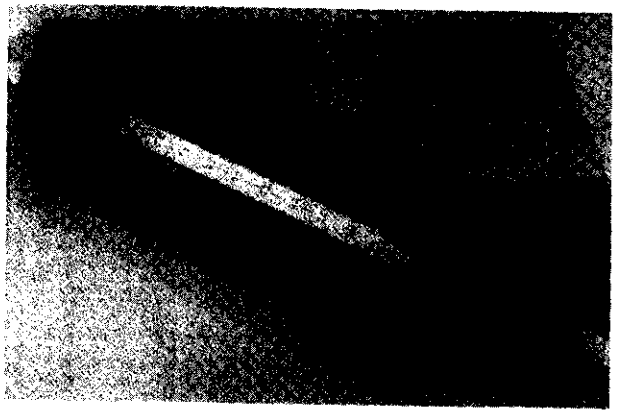

Fig. 1 A superconducting quadrupole coil. The scale is in inches.

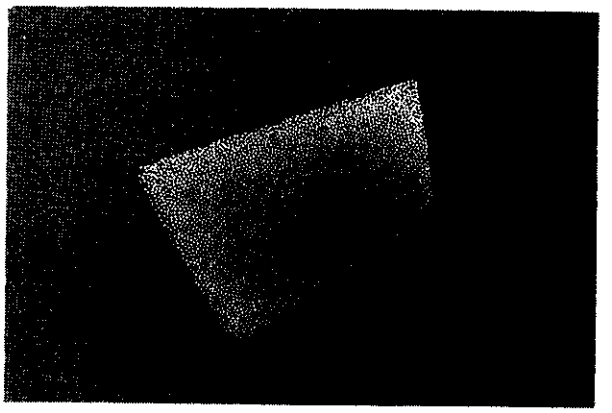

Fig. 2 Cross section thru a quad coil.

installation, all four coils had identical resistances, including the previously shorted one. Additionaly when 40 mA at 175 V was passed thru all the coils, the measured magnetic field had a quadrupole symmetry to better than 2%, the limit of our apparatus at such low fields. This confirms that the coil no longer has a room temperature short.

To further check, the three other shorted coils were remeasured and found to be still shorted. They were then cold shocked in liquid nitrogen and retested. All were found to be unshorted. The results are listed in table 1. Note that coil number 5, which was installed in the quad could not be inductance checked, and that the other three coils were measured at a slightly higher ambient temperature (1°C is a 4Ω change in resistance). That all five coils responded in the same way, and that previously unshorted coils did not change their resistances or inductances indicates that the shorts are indeed gone.

TABLE 1: Resistances and inductances of coils at room temperature.

	RESISTANCE (OHMS)		INDUCTANCE (H)	
COIL No.	before	after	before	after
5	730	959	1.43	--
6	850	975	1.21	6.45
7	943	970	1.81	6.45
8	950	971	4.17	6.71

The coils appear to be shorted during the winding process, with a tension on the wire of 1-2 lbf, since the resistance is low even before the coil is cured. Since the sides are straight only the ends are under tension, and this is where the maximum number of wire crossings occur. We believe that the shorts result from compression of the insulation at these crossings and that the cold shocking relieves the stress at these points, removing the short. The coil stress can be viewed as being frozen in during the high temperature curing cycle and that the contraction during cooling relieves this stress. Of course, one might expect that upon warming of the coil the shorts would reappear, but this does not seem to be the case. A similar effect occurs during training, that is, an irreversible process. We also do not know whether this process will work for all potted coils, or just ones having large numbers of turns and considerable stress concentrations at a few points, as our coils do. However, the cold shocking process may be a simple solution to remove shorts from potted coils.

REFERENCES

1. A.R. Zeller, et al, Proc. Tenth Int. Conf. on Cyclotrons and their Applications, 1984, p 79.

GAMMA-RAY DETECTOR BEAM-PHASE MEASURING PROBE-TESTS AND IMPLEMENTATION

M. Fowler, B. Milton, M. Maier, R.M. Ronningen, and J. Yurkon

The K500 cyclotron has few penetrations in its yoke for diagnostic equipment, and these are limited in size by the small space between the main coils. Thus, auxiliary devices must also be small as well as be impervious to the large magnetic fields within the cyclotron, or to the strong fringing fields outside the yoke. Such constraints are also imposed on diagnostic equipment for the K800 cyclotron, too.

One example of useful diagnostic equipment is a beam- phase and phase-width detector which can measure these quantities as a function of radius.

For the K50 cyclotron a fast plastic scintillator detector[1] was developed to measure the arrival time, with respect to rf, of gamma rays from reactions from the probe intercepting the beam. This detector was external to the cyclotron. The same detector was then tried during the initial operation of the K500, but its usefulness was severely limited by several factors. First, small penetrations collimate the detector's view to only several inches of probe travel. Secondly, the penetration that is readily available views primarily the ion source region. Thirdly, the gamma-rays from the beam hitting the probe are very difficult to discern from other highly active sources of gamma rays within the cyclotron.

We next tried to get the detector close to the beam chamber by epoxying a plastic scintillator on a long glass rod coupled to a glass vacuum porthole window and photomultiplier tube. The third problem discussed above still remained. Because the most useful phase information comes from the last several inches of radius before extraction one may employ the "viewer probe" rather than the main probe as it intercepts the beam in the last six inches of radius. We then designed[2] a scintillator detector integral to the viewer probe and its drive mechanism. While the above problems would by the cumbersome magnetic shielding for the PMT.

Concurrently with the latter design it came to our attention that PIN silicon photodiodes can be utilized as gamma-ray detectors directly, albeit their usual employment is as PMT replacements. The advantages of PIN diodes are that they are compact, have low noise due to small capacitance and resistance, and are capable of fast risetimes. We are currently using the Hamamatsu series S1722 in our prototypes. The sensitive area is 13.2 mm^2, the junction capacitance is 12 pF, and the maximum risetime is 1 nsec.

One was first tested for performance in a high magnetic field. Using a light pulser the pulse-height amplitude changed by only about 20% when placed into the full field of the K800 magnet. A second test was made using the external beam intercepting a copper finger in which the PIN diode was placed. While little time could be given to this test, the diode detected gamma rays only when the beam intercepted the finger, and not when the beam was sent to a beam dump only six inches away. The time response appeared to be as good as the fastest scintillator used to look at the time structure of the external beam (barium flouride). Both of these tests used a preamplifier design by H.J. Beeskow of GSI-Darmstadt.

A prototype of the PIN diode detector with an integral preamp has now been built and will soon be tested in the external beam. It is shown in Fig. 1. A new viewer probe for the K500 is also now ready for installation and can

Fig. 1 Prototype PIN diode gamma-ray detector system for phase measurements. The PIN diode is described in the text. The preamplifier is based on a wide-band amplifier IC by NEC Corporation, μPC1651G. It has an amplification factor of nine. The cables are standard-sized lemo cables.

accomodate this detector. If the prototype works well, it or an improved version can be used for phase measurements and diagnostics within two months. And, such a detector would certainly prove useful for the K800 as well.

References

1. P. Miller, H. Blosser, W.S. Chen, J.F.P. Marchand, and G. Stork, MSU Cyclotron Laboratory Annual Reports 1974-1976, p.112.
2. B. Milton, M. Fowler, J. Kuchar, and R.M. Ronningen, Proc. Tenth Int. Conf. on Cyclotrons and Their Applications, April 30-May 3, 1984, East Lansing, MI,IEEE 1984, p.55.

ANALYSIS OF LOW-TEMPERATURE IMPURITIES IN He BY GAS CHROMATOGRAPHY

Jon C. Batchelder and Wm.C. McHarris

In liquid-He cryogenic systems almost any foreign substance becomes a bothersome impurity, in that it will solidify and stop up the lines. Luckily, most substances can be removed fairly easily by using cold traps and micro-porous filters. However, here at NSCL we have experienced problems with H_2 and Ne impurities, both of which make their way through the traps and filters. We are developing several systems for analyzing for these in the presence of He. Here we report on the status of using gas chromatography.

None of these gases is strongly adsorbed, so specially packed, long columns are needed, and low temperatures may be required for clean separations of minute quantities.[1] We have been using a refurbished model 90P-3 Varian Aerograph gas chromatograph,[2] together with a column packed with 60-80 mesh #5A molecular sieve. Our preliminary results have been obtained with an 8-foot column at room temperature, although we have now extended the column to 16 feet and plan to extend our measurements down to lower temperatures.

Samples consisting of about 2 cm^3 STP are introduced into the chromatograph by means of a gas syringe. One of the major problems was to find the carrier gas that would yield the best separation. We have found Ar to work quite well, and an example of a H_2-He separation, is shown in Fig. 1.

Gas chromatography has proven to be a relatively straightforward, inexpensive analytical tool for routine analyses of these light, low-boiling gases. The question that remains is whether or not it can be made sensitive enough to detect H_2 and/or Ne as parts-per-million impurities in the feed He. We are now working on this problem.

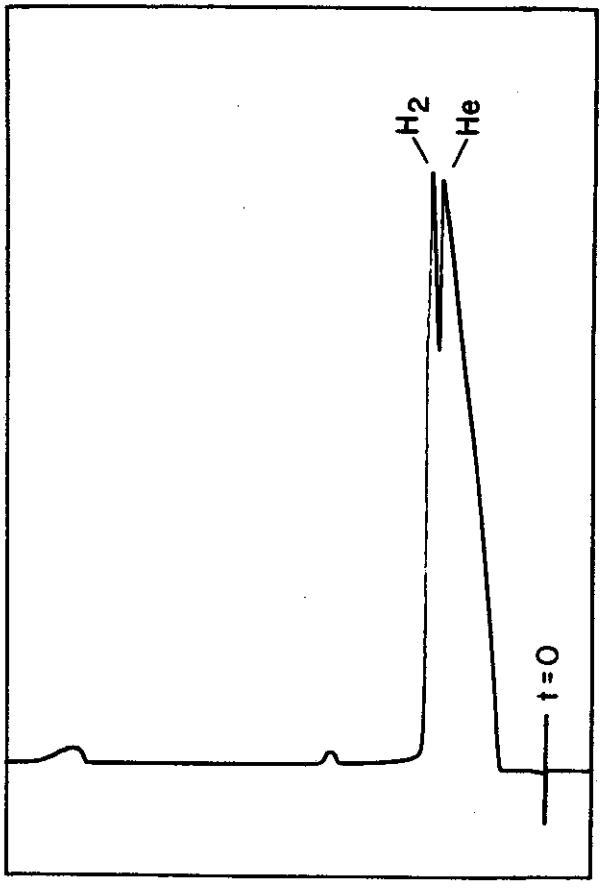

Fig. 1 A H_2-He gas chromatographic separation, using an 8-foot column packed with 60-80 mesh molecular sieve #5A, Ar carrier gas, 40°C, flow rate of 40 ml/min. Retention times: 1.9 min for He, 2.0 min for H_2. (N_2 and O_2 peaks can also be seen in the spectrum.)

References

1. P.G. Jeffrey and P.J. Kipping, Gas Analysis by Gas Chromatography, Pergammon Press, Oxford, 1972, Chap. 7.
2. We thank the MSU Chemistry Department for giving us this gas chromatograph.

INDUCED α ACTIVITY WITH THE K500

M.L. Mallory

In 1983, the Oak Ridge Ischronous Cyclotron (ORIC) was contaminated by the α emitters ^{210}Po and ^{208}Po. Subsequent studies discovered that this activity was produced by the acceleration of a heavy ion beam that exceeded the fusion barrier on tantalum and the target-projectile atomic mass exceeded the mass number of the actinides isotopes. The accelerator extraction septum was made of tantulum.

We have now studied this activation problem for the K500 cyclotron. The results of the study are summarized in Figure 1 and indicate that there exists an activation window that opens in the acceleration process using the K500 when the ECR is the ion source. In Figure 1, the shaded area of charge vs mass indicates where the α activation region occurs. The double shaded area indicates the region where molybdenum has replaced the tantalum accelerator components. This substitution considerably reduces the activation region and is being implemented in the K500. The Penning ion source upper charge limit has been plotted and it falls below the activation zone. With higher K cyclotrons (e.g. the K800) and higher charge state ion sources, (ECR, cyclotron injection, tandem injection), this activation region will be encountered and must be handled with appropriate safety measures.

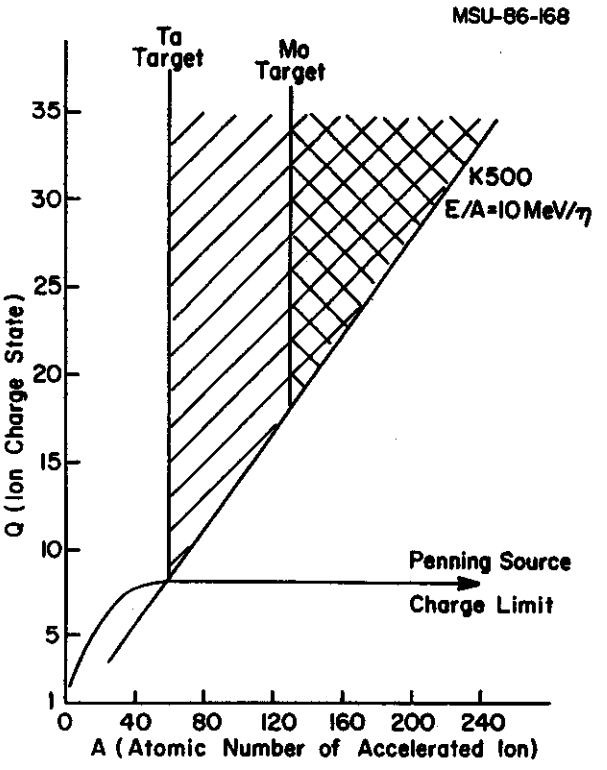

Fig. 1 The accelerated ion charge state versus it's atomic number is plotted for the K500 cyclotron. The shaded area is where induced α activity ion occurs within the accelerator. The normally obtained Penning ion source charges are below this shaded area.

RADIOACTIVE ION BEAMS

M.L. Mallory

In a previous annual report, a study to build a radioactive ion beam separator in the beam line was reported. This separator is presently on hold. It has since been realized that the K500 cyclotron can be utilized as an isotope separator for a given class of radioactive ion beams. These beams are called analogue radioactive ion beams and some are listed in Table I.

The concept of cyclotron analogue beams has been around for many years and means that the charge to mass ratio is nearly equal between two different ion species. For the radioactive ion beams, it means the charge to mass ratio is nearly equal between the initially accelerated beam from the ion source and the radioactive beam produced by the initial beam at a target located in the cyclotron. How near to equal the charge to mass ratio must be for successful production of radioactive ion beams depends on the location of the target in the cyclotron. For instance, if the target is located on the last normal turn, the difference may be quite large. Figure 1 illustrates the computed phase history for converting a $^{6}Li^{2+}$ beam to $^{3}H^{1+}$ at a radius of 15" in the K500 cyclotron, where the trim coils are adjusted to correct for the small charge to mass ratio difference. This calculation shows that the above beam can be successfully produced and accelerated in the K500.

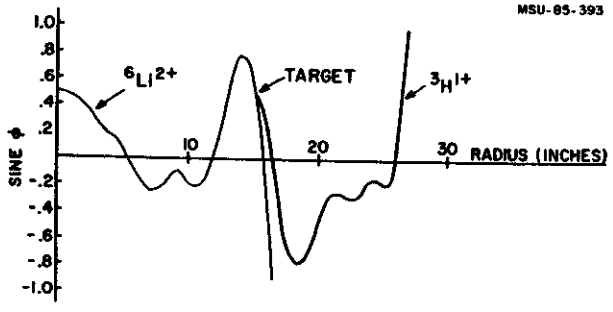

Fig. 1 The completed sine phase curve for $^{6}Li^{2+}$ going to $^{3}H^{1+}$ with a final energy of 30 MeV/u is shown. The fragment producing target was located at 15" for this calculation.

Another criterion for acceptance of the fragmented ion beam into the accelerator phase space is that the radioactive ion has the same velocity or energy/nucleon as the impacting initial beam. Figure 2 energy spectrum of a carbon beam shows an after fragmentation which suggests that some fraction of the fragments has the same energy/nucleon as the incident energy/nucleon of the primary beam and thus that

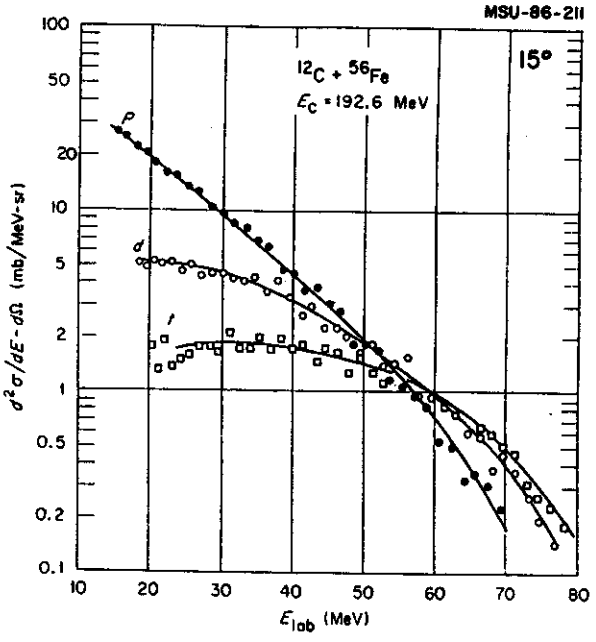

Fig. 2 The light fragment from a carbon beam interacting with a target are shown. The energy/nucleon for the triton of the accelerated beam. These fragments have a chance of falling within the cyclotron acceptance phase space, after being produced at a target within the cyclotron.

this fraction of the radioactive ions will be accelerated further in the cyclotron.

Table I

Analogue Radioactive Ion Beams

Primary Beam	Fragment Beam	Lifetime
$^{6}Li^{2+}$	$^{3}H^{1+}$	12.3y
$^{12}C^{4+}$	$^{6}He^{2+}$	805 ms
$^{16}O^{4+}$	$^{8}He^{2+}$	119 ms
$^{16}O^{6+}$	$^{8}Li^{3+}$	844 ms
$^{18}O^{6+}$	$^{9}Li^{3+}$	177 ms
$^{22}Ne^{6+}$	$^{11}Li^{3+}$	8.7 ms
$^{22}Ne^{8+}$	$^{11}Be^{4+}$	13.8 s
$^{24}Mg^{8+}$	$^{12}Be^{4+}$	24 ms

Estimates of the beam intensity expected for these radioactive beams have been made, but with large uncertainties. An experiment to determine the cyclotron yield of a $^{6}He^{2+}$ beam is planned and will yield better estimates for all analogue radioactive ion beams.

Although there are stringent requirements for producing analogue radioactive ion beams in the cyclotron, there are also some advantages. The initial beam intensity can be raised to the ion source limit, which can be 2 to 3 orders of magnitude greater than the cyclotron extracted beam. Secondly, this method of producing these beams can be easily implemented. Thirdly, this beam can be directed to all of the existing target stations, thereby making it possible to use the full power of the laboratory experimental tools. If a pure radioactive beam is desired, the separation power of the ischronous cyclotron can resolve the beam, with a corresponding decrease in intensity. Calculations and experimental measurements are being planned to obtain more information about this method of making radioactive ion beams.

ACCELERATOR APPLICATIONS

H.G. Blosser

In November 1981, publicity concerning the start-up of the K500 cyclotron came to the attention of a medical group in Detroit that had been working to obtain a cyclotron for neutron therapy. Comments in the newspaper article as to smaller size and reduced cost of the superconducting cyclotron led the group to ask the Laboratory if a superconducting cyclotron might be a more attractive neutron therapy system than a conventional cyclotron. Responding to this request, a modest study was set in motion which led to some quite appealing conclusions -- the superconducting cyclotron could indeed achieve a major reduction in the size and complexity of a neutron therapy system. The primary advance would come from mounting the cyclotron directly on a rotating gantry so that neutrons produced in an internal target could be directed at a patient from any desired direction. This eliminates the beam extraction system, the beam transport system, and the beam swinger system, all of which are complicated and expensive components of a conventional room temperature neutron therapy system. The cyclotron is also exceedingly simple compared to the variable-energy, multiparticle, research cyclotrons, which the Laboratory is customarily designing, because the neutron cyclotron involves only one projectile and one energy. The rf system thus operates at a single frequency and no field shaping corrections are needed in the magnet. One novel requirement, which involves some intricacy, is the need for the helium vessel to continue to function as it rotates on the gantry through a full 360 degrees -- a design having this capability has been worked out and experimentally tested in a mock-up vessel.

A few months of initial design studies established the basic characteristics and workability of a possible neutron therapy system. An extended period of negotiations followed between MSU, Harper-Grace Hospitals of Detroit, and the National Science Foundation. From the beginning it was recognized that if the project was successful, it would probably be an element of a future commercial enterprise. The three organizations involved were just beginning to develop policies aimed at encouraging spin-off of research based technical developments into commercial enterprises. Negotiations as to an appropriate organizational format for handling such a project were then significantly prolonged by the desire of the several institutions to arrive at an arrangement which would be an appropriate model for future spin-off situations and which would be consistent with institutional policies which were then in the midst of being developed. These negotiations culminated in September 1984 with the signing of an agreement between MSU and Harper-Grace Hospitals to proceed with construction of such a cyclotron, with the National Science Foundation concurring in the arrangement and allowing use of NSCL facilities in the project on a non-interfering basis relative to the main NSF program. The MSU/Harper agreement provides for 100% funding of the project by the hospital, including full overhead, etc., in accord with normal MSU procedures for research projects. Specifications on expected performance and anticipated total cost were based on the prior MSU study, and the achievement of these goals was recognized as being on a best effort basis. If there are unexpended funds at the end of the project, they will be shared between the hospital and NSCL, with no restriction on the use of such funds by the Laboratory. The project is under the direction of H. Blosser who

will work on the project on a 5% of full-time basis, assisted in special situations by other Laboratory personnel up to a total level estimated to be 3,000 man hours. Primary manpower for the project is furnished by the hospital in the form of a technical team of approximately five full-time persons who work at NSCL under Blosser's direction. Rights to commercialize the venture pass to the Hospital (following a pattern which is normal at MSU for fully funded research enterprises) but with the University retaining royalty rights on future commercial sales.

Implementing the above agreement, Harper-Grace Hospital organized a small corporation, MedCyc, and contracted with this corporation to provide the technical group. Harper also passed through to this corporation, in exchange for stock, the manufacturing rights which it obtained under its agreement with MSU. The corporation also involves participation of a Michigan venture capital group with expertise in management of start-up companies and participation by a number of Laboratory staff members as shareholders. The project has been moving forward under this format since September 1984.

Detailed design of the neutron therapy cyclotron considered three beam options, namely 50 MeV protons, 75 MeV ^{3}He, and 50 MeV deuterons. Deuterons were ultimately selected primarily because the rf frequency is in the commercial fm transmitter band (for the desirable, high-energy-gain, third harmonic mode). Pre-engineered transmitter packages for this band are readily available from several commercial vendors and maintenance for such transmitters is broadly available throughout the country. The magnet required for the deuterons is somewhat more massive, namely 25 tons compared to 15 tons for the proton or ^{3}He magnets, but remains compatible with a reasonable 360° rotating support system. Deuterons, moreover, have significant targeting advantages, giving a much higher neutron yield than either of the other projectiles. Higher forward peaking of the neutron yield from the deuteron reaction reduces activation of machine components and a reduced low-energy-tail in the deuteron induced neutron spectrum is thought to help avoid skin overdose during treatment.

Construction of this cyclotron is now in midstream, with all major parts on order from various vendors and with winding of the main superconducting coil about to begin. The cyclotron magnet is expected to be ready for first operating tests in the spring of 86 and ready for rf and beam testing a few months thereafter. Following these tests, the cyclotron will be transported to the hospital in Detroit and the MSU project will end, as the hospital technical group takes over responsibility for installing the cyclotron in Detroit and starting up the machine there.

More recently, the Laboratory has become involved in another medical application study in response to inquiries from the Harvard Cyclotron Laboratory and from Fermilab as to whether superconducting cyclotrons might constitute a competitive accelerator solution for providing proton beams for radiotherapy. In this latter application, a beam energy of 250 MeV is desired with a current of 20 nanoamps. A small study, involving several man-months of total effort, concluded that a superconducting synchrocyclotron might well be the most attractive accelerator for this application. The beam current requirement and the beam quality requirements are compatible with routine synchrocyclotron performance and superconducting techniques make the accelerator smaller and less costly.

A likely superconducting synchrocyclotron design would utilize a 5.5 tesla central field and an rf system modulated over the range 65 to 85 MHz. Extraction of beams from synchrocyclotrons is normally accomplished by "regenerative" extraction, an entirely magnetic

technique. It appears that this technique can continue to be utilized in the high magnetic field regime but quantitative calculations remain to be done to firmly establish this.

More recently we have learned that a group at the SIN Laboratory in Switzerland is interested in developing a cyclotron for proton radiotherapy and NSCL/SIN discussions are in process regarding a possible joint project in which MSU would undertake design studies of the magnet and SIN would undertake design studies of the rf system. Such a project could ultimately evolve into a pattern paralleling the neutron facility, depending on whether some medical organization is able to obtain the necessary funds.

The laboratory is also participating in an ongoing adhoc national study aimed at comparing the advantages of various types of accelerators in the proton radiotherapy application. Several meetings were held on this topic in 1985, with initial meetings at Fermilab, sponsored by Fermilab, and since then sponsored by an adhoc panel, the Proton Therapy Cooperative Group (PTCOG). The Laboratory's participation in this study provides an element of balance, since other accelerator laboratory participants are dominantly from synchrotron backgrounds and the NSCL group is the only one involved in study of the synchrocyclotron option.

Overall, the applications program has brought a great deal of favorable public comment and public appreciation of the Laboratory's program. Appreciation of possible benefits of nuclear physics spin-offs has been greatly enhanced in the mid-Michigan and Detroit areas. The applications program is also enthusiastically supported by a number of members of the Michigan congressional delegation. We believe this enhances political support for the overall national nuclear science program. In summary, we feel the applications program is important and useful, provided it is kept at a level which does not significantly impede or delay the mainline programs of the Laboratory.

CENTRAL REGION STUDIES FOR THE MEDICAL CYCLOTRON

J. Griffin and F. Marti.

In this contribution we summarize the design studies of the central region of the medical cyclotron under construction at this laboratory. The medical cyclotron project is described in H.G. Blosser's contribution "Accelerator Applications" in this Annual Report.

This cyclotron is a fixed energy machine, designed for 50 MeV deuterons, running in third harmonic. The central field is 46.5 kG and the RF frequency is 106.38 MHz. Transmitters for this band are commercially available, a desirable feature.

Running in third harmonic eliminates the problems associated with neutralization of the coupling among the three dees that exists when running in first or second harmonic. But it creates problems due to the long transit time of the ions between source and puller. The puller voltage reverses sign before the ions have crossed the first gap. The way to avoid this difficulty is to decrease the distance between source and puller, decreasing the voltage accordingly. Our numerical studies showed that a voltage of 40 kV applied over a distance of 0.4 cm gave a reasonable energy gain and transit time. This electric field is higher than the one we reliably achieve in our K500 cyclotron (although the voltage X electric field product is smaller). It was decided to test the possibility of achieving the required voltage with an actual ion source in the K500. As this test showed that it was possible to run 40 kV over 0.4 cm in the source to puller region[1] we continued the design with that electric field limit in the rest of the central region.

The full vertical gap inside the dees and the pole tips is 1.5 inches. The pole tips will be copper-plated and a liner plate will start at approximately 3.5 inches and taper the gap towards the center of the cyclotron, reaching a full height of 0.375 inches at the inner radii. The dees will be similarly shaped in the gaps. The purpose of this reduction in the gap is to decrease the electric field penetration into the dees and dummies. All three dees are joined at the center by a common copper nose.

An equipotential map is shown in Fig. 1, where the large horizontal gap width becomes obvious at radii of 5 cm and larger. The ion source is the small circle with a diameter of approximately 0.6 cm. The electric potential was computed using TRIUMF's RELAX3D, a relaxation code developed by C. Kost[2].

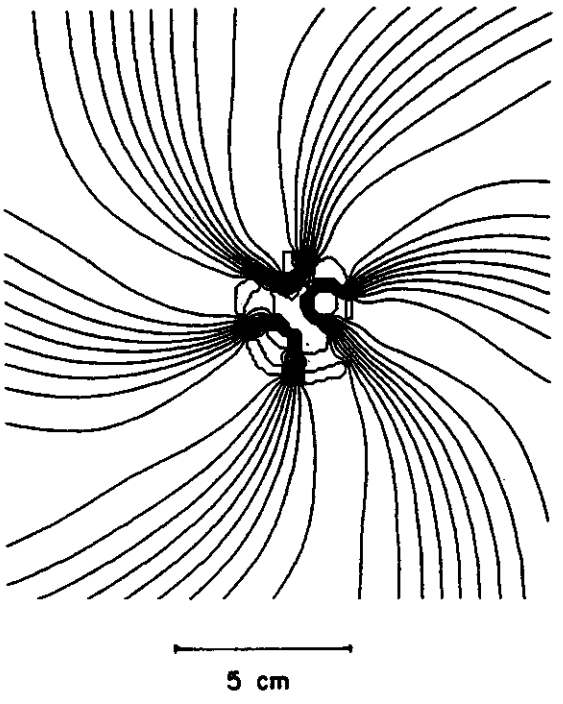

Fig. 1 Equipotential plot of the electric field in the medical cyclotron central region. The small circle near the centre is the ion source with a diameter of 0.6 cm. The source to puller gap is 0.4 cm and the dee voltage 40 kV. The equipotentials corresponding to 10,20,...and 90 percent of peak voltage are drawn.Note the fast increase in radial gap width with radius.

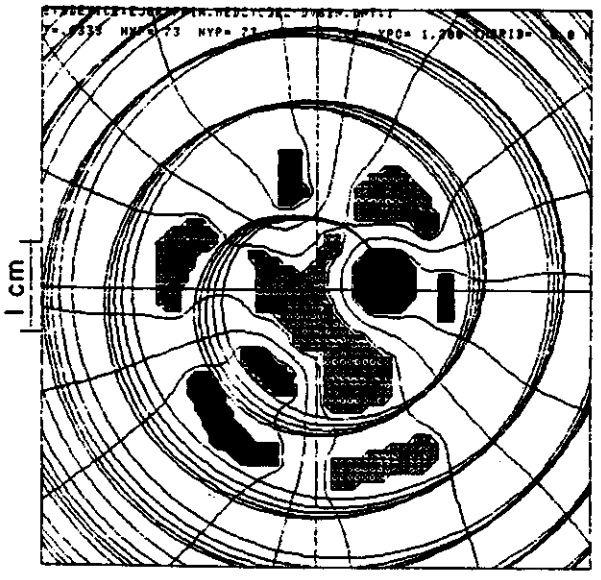

Fig. 2 Radial plot of five different orbits. The displaced rays start ±4 and ±8 RF degrees around the central ray. The solid areas correspond to the ground electrodes and the cross-hatched areas are the high voltage electrodes. The cross-hatched grid shows the grid size used in the relaxation calculation. The 10,50, and 90% equipotentials are drawn.

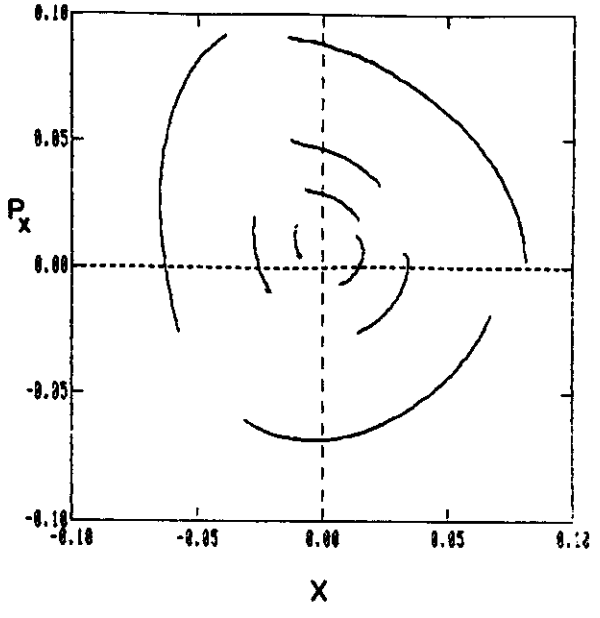

Fig. 3 Displacement with respect to the equilibrium orbit for turns 18 through 54 plotted three times per revolution. We plot here the central ray (the 3 line segments closest to the origin) and the two extreme rays shown in Fig. 2. The units are inches for both x and p_x.

The motion of the ions was studied with our CYCLONE code in a three dimensional electric field. The motion within two relaxation grid spaces from the ion source was computed using an analytic treatment. From there on numerical integration in the relaxed field was used. Fig. 2 shows the results of such computations. The solid areas correspond to the ground electrodes and the cross-hatched ones to the dees. Five orbits are plotted, corresponding to the central ray which leaves the ion source at τ=230° (where V_{dee}= Vo Sin τ) and to ions starting at the source +/- 4 and 8 RF degrees away from the central ray. The centering of those orbits can be seen in Fig. 3 where we plot the p_x vs x motion with respect to the equilibrium orbit for the central ray and the +/- 8 RF degrees trajectories.

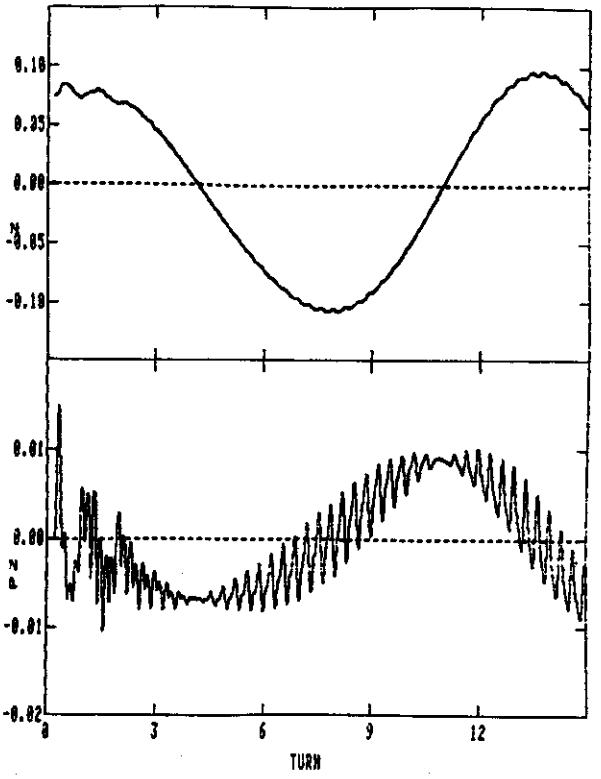

Fig. 4 Vertical motion plots, z and p_z (both in inches) vs. angle for an ion that starts 0.075 inches above the median plane. The entire motion plotted here is calculated in a three dimensional electric field.

Figs. 4 shows typical results of the vertical motion studies. For example, z and p_z vs turn number for an ion starting with a z displacement of 0.075 inches and no p_z.

References

1. H. Blosser, private communication.
2. C. Kost, TRIUMF, U.B.C. Canada.

STATUS OF CONSTRUCTION OF THE 4π DETECTOR

J. van der Plicht, G. Westfall, L. Morris, M. Maier, S. Tanaka, J. Yurkon, D. Swan, M. Williams

We have built and succesfully tested a prototype detector for the 4π array. A report of tests and experiments with this device has been published[1]. The 4π array will consist of 30 detector modules, 20 hexagons and 10 pentagons. Each module consists of a Low Pressure Multi Wire Proportional Counter (MWPC), a Bragg Curve Counter (BCC) and a Scintillator telescope (phoswich detector) made from a combination of fast and slow plastic - see Fig. 1.

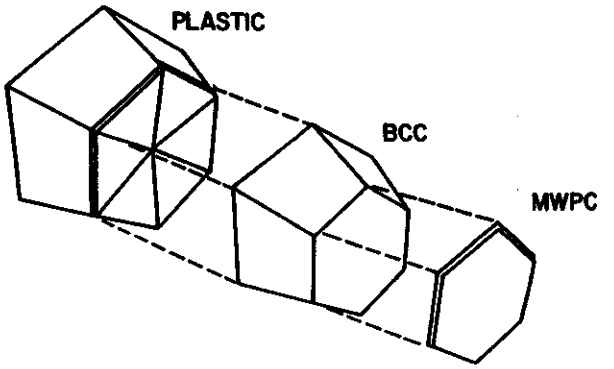

Fig. 1 Schematic representation of one of the 30 modules that will make up the 4π array.

For the production style detectors, we have built two MWPC detectors, a hexagon and a pentagon. The design and construction is much more complicated compared with the prototype detector and any regular PPAC (Parallel Plate Avalanche Counter) or MWPC. The walls of the counters are only 0.125" (3.2 mm) thick G10. Gas lines and cabling obviously cannot stick out of the detector as is usually the case since this does not allow close packing. Therefore we will use flat cable laid in 0.031" (0.8 mm) grooves in the sides of the counters. The gas is supplied by tubing routed through the sides of the scintillators and Bragg Curve Counters.

For the BCC, we had to build a second prototype. Tests revealed that the detector body and glue joints to the scintillator can withstand an overpressure of 2 atmospheres without leakage (the working pressure is around 500 torr). The scintillator telescopes are presently in production at Bicron,Inc.

The concept of the vacuum vessel is shown in Fig. 2. The whole 4π detector can rotate around the beam axis so that each module is easily accessible. We expect the vessel to be completed by mid 1986. The 4π detector modules form a truncated icosahedron or soccerball geometry. The soccerball, with a diameter of about 6 feet has been constructed and is shown in Fig. 3. The soccerball will be sealed with

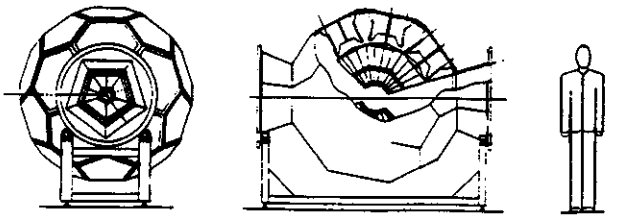

Fig. 2 Concept of the 4π array detector vessel.

RTV; we selected the material based on a test box built to perform tests on various kinds of sealant. The vacuum system (pumps, gate valves, bellows etc.) will consist of NW250 (10 inch diameter) components. A set of pumps and gate valves was purchased from Dupont.

For the 60 gas counters, we need to control the pressure and flow of the gas. A prototype gas handling system has been built, based on the 68701 microprocessor. It reads the pressure in the detector with a transducer, and controls the solenoid valves and the servovalve. The pressure is read by an ADC with 14 bit resolution; a digital feedback loop is used for pressure control. We are planning to use one system like this for every group of 5 detectors hooked up in parallel.

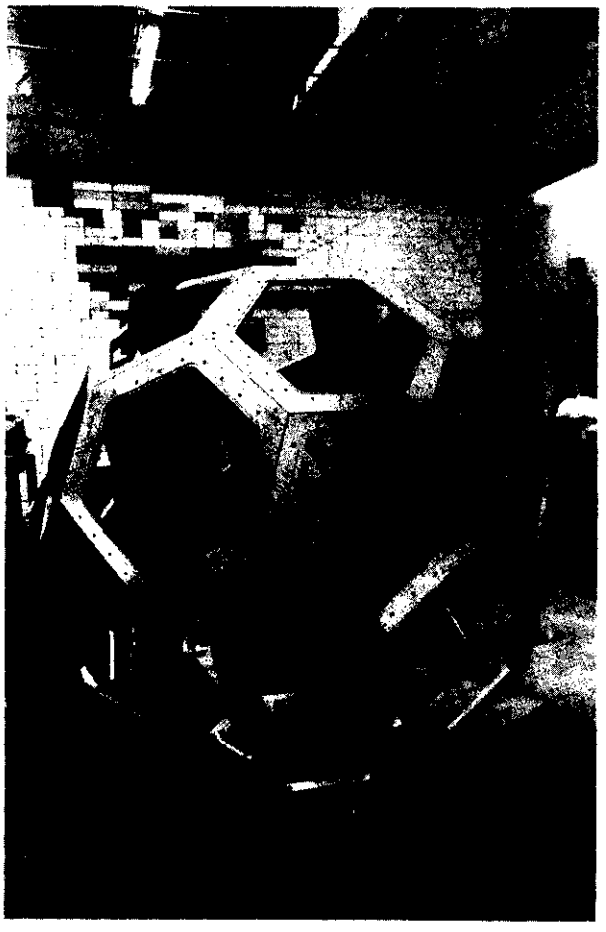

Fig. 3 The support structure (soccerball) for the 4π array.

For monitoring of the scintillator phoswich detectors, a laser system will be used. Light from a Nitrogen laser with a wavelength of 337 nm will be distributed by a mirror to bundles of fiber optics cables, routed to the scintillators.

A large evaporator has been built to ease the upcoming mass production of metallized foils. With its system of well thought out masks, it is capable of evaporating 2 detector foils at the same time. The evaporator will also be used to aluminize the front surfaces of the scintillators, which will serve as anodes for the Bragg Curve Counters.

For the datataking electronics, the major purchase orders are placed. For the 30 MWPC's, the 30 BCC's and 170 Phoswiches, a total of 550 ADC - and 260 TDC channels are needed. We will use the Lecroy (ECLine) FERA system. The scintillators will be read out with 3-inch diameter photomultipliers.

During the recent shutdown of the K500 cyclotron for ECR installation we installed a beamline and wallplug in the wall behind the Enge spectrograph. The 4π array will be placed in a temporary vault adjacent to the north vault for the laboratory's phase 1.5 operation. We expect some modules to be ready for use with the K500 running with ECR beams by the end of 1986.

References

1. G.D.Westfall, J.E.Yurkon, J.van der Plicht, Z.M.Koenig, B.V.Jacak, R.Fox, G.M.Crawley, M.R.Maier, B.E.Hasselquist, R.S.Tickle, and D.Horn, Nucl. Instr. and Meth. A238 (1985) 347.

DEVELOPMENT OF CCD CAMERAS TO RECORD STRAMER CHAMBER EVENTS

S.P. Angius, G.M. Crawley, C. Djalali, D. Fox, M. Maier, R. Tickle[a], T. Wallaert,and G. Westfall

In a preliminary run at the LBL streamer chamber, the CCD-camera system developed during the past year was used to record central collisions of 100 MeV/nucleon ^{93}Nb on a ^{93}Nb target. The digital output of each of the three CCD's, consisting of almost half a Mbyte of information, was processed on-line by a MC68000 microprocessor, which subtracted a previously stored background, applied a low threshold cut and compressed the remaining non-zero pixels through a bit-mask-type encoding. The total amount of data was thereby reduced by a factor of 3 to 5, thus providing sufficient compression to record and write to tape one event per Bevalac spill.

The greater sensitivity of the CCD's, as compared to photographic film, allowed operation of the streamer chamber at a lower voltage, where it approaches the avalanche, rather than the streamer, mode, thus improving the charge-identification capability of the chamber.

An example of a picture taken during this experiment is given in Fig. 1. One can see how some areas are obscured by flares which would make a computer-assisted recognition of the tracks a very difficult task. One of the advantages of obtaining completely digitized data on tape is the possibility of using digital processing for track enhancement, to make the tracks more visible. The results of such a procedure are displayed in Fig. 2, where the event shown in Fig. 1 has been computer-processed using a program which calculates the double azimuthal derivative of the intensity. A track-recognition code can now scan this image to find the tracks. The points in Fig. 2 are the result of this program, after the operator has corrected the output for omissions and other possible errors. The track coordinates were then used as input for a three-dimensional

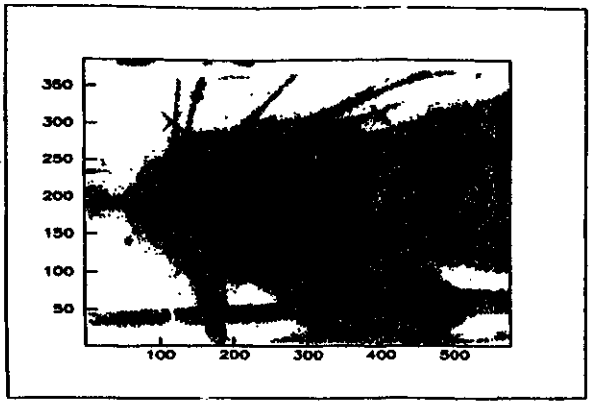

Fig. 1 CCD image of a central collision of Nb on Nb.

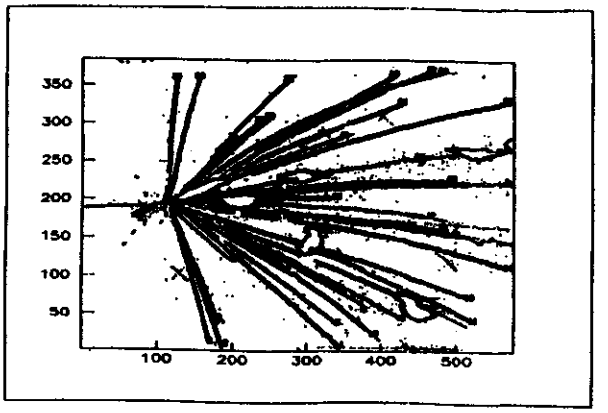

Fig. 2 Image-enhanced representation of the event shown in Fig. 1. The dots on the tracks are the result of a track-recognition program.

geometrical reconstruction program (TVGP), from which rigidities,dip and azimuthal angles, and track lengths were extracted for each particle.

The other information which can be extracted from CCD pictures is the intensity of the tracks. As the fragments lose energy in the gas of the chamber, the ionization of the gas, and therefore the intensity of the light emitted, depends on the charge and the momentum of the particle. An intensity histogram for a cut along the Y-axis of Fig. 1, for X= 200, is

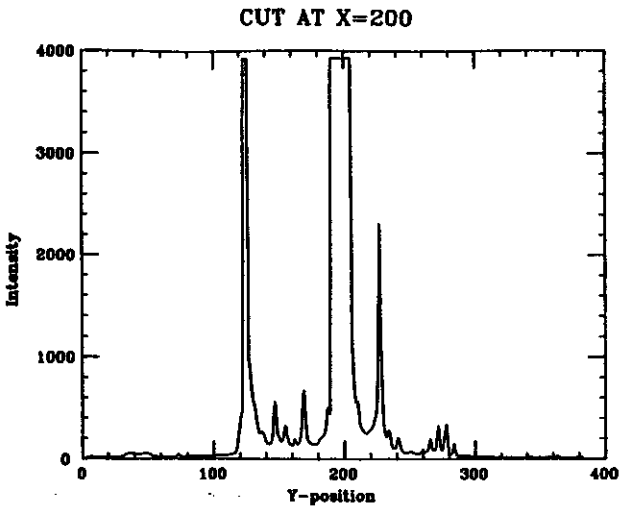

Fig. 3 Intensity histogram of a vertical cut in Fig. 1.

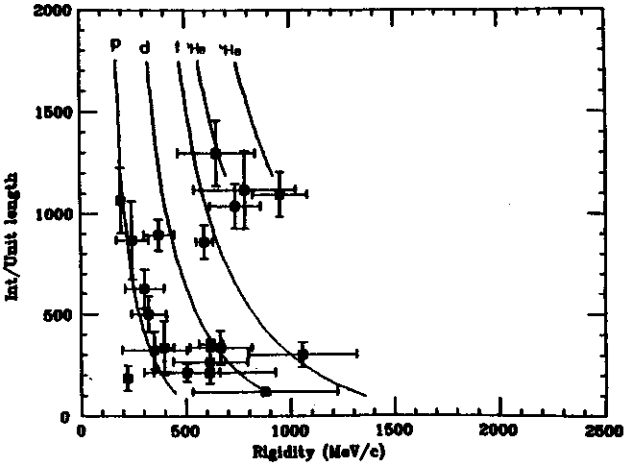

Fig.4 Example of a particle identification plot for some of the tracks in Fig. 1.

shown in Fig. 3. Peaks of heights from about 5 to 4000 can be seen, showing the large dynamic range of the CCD's. This, combined with the linear response to light of the devices, should give a better separation between different ions, and allow the identification of high-Z particles. A preliminary example of a particle-identification plot is shown in Fig. 4. Here, the average intensity per unit length, calculated over about 2 mm, is plotted as a function of the particle rigidity, obtained from TVGP. The very intense tracks corresponding to ions heavier than α-particles have not been included in this plot. The comparison with the solid lines, obtained from theoretical energy-loss calculations, indicates that p,d,t,^{3}He, and α-particles can be separated, even at this preliminary stage, where large uncertainties are present for both the intensities and the rigidities. Alternative methods for using the intensity information to performe particle identification are under study.

A new experiment, performed with 100 and 200 MeV/nucleon Nb beams on Nb, has been carried out recently, and over 1000 central events have been recorded at each energy. The analysis of the data collected during this run is in progress. A better knowledge of the system and of the requirements for obtaining good quality data has help in improving the performance of the chamber during this recent run. Also, more up-to-date information about the geometry of the chamber should reduce the uncertainty in the estimate of the rigidities.

---

a University of Michigan, Ann Arbor.

InSb AS A γ-RAY DETECTOR

Wm. C. McHarris, R. Ronningen, and M. Maier

Since the introduction in the early 1960's of Ge(Li) detectors for γ-ray spectroscopy, almost constant efforts have been expended to enlarge them, make them more uniform, and improve their stability; this in addition to increasing their resolution and peak-to-Compton ratios. Much of the recent work has centered on elaborate Compton-suppression spectrometers, using NaI(Tl) or BGO ("bismuth germanate") shields[1,2] and on electronic pulse-shape discrimination techniques[3,4] to correct for damage and non-uniformities in charge collection. Although present technology has quite a way to go to attain the theoretical limits on resolution and peak-to-Compton ratios, we are witnessing signs of diminishing returns with respect to effort and expenditure versus improvement. Thus, it is worth while investigating possible alternative materials to Ge for fabricating high-quality γ-ray detectors.

A significant amount of research has gone into investigating other semiconductors.[5] Most of the effort, however, has gone into investigating large band-gap materials that would serve as useful compromises between Ge and NaI(Tl).

Our interests lie in the opposite direction -- investigation of small band-gap semiconductors (with a large Z, if possible) that could provide even better resolution and peak-to-Compton ratios than Ge, but, on the other hand, most likely would be even more tricky and cumbersome to use. Of the possible semiconductors, the III-V compound InSb stands out in all respects. It could potentially replace Ge as the "γ-ray detector of the next generation," but it will require considerable technological development before its potential can be realized. In principal, InSb should make a superior γ-ray detector. Since the photoelectric effect scales as Z^5, the InSb effective Z of 50 results in an efficiency (per mole) of 9.3 times that of Ge and a linear stopping power somewhat higher if the differences in densities are folded in. Also, single-event Compton scattering scales as Z, so if the resolutions of InSb and Ge were comparable, InSb would have a peak-to-Compton ratio 6 times better than Ge -- this on the basis of Z alone. (And, of course, assuming comparably sized detectors, which is not a reality at this time.)

The resolutions are not comparable, however, for the InSb band gap is much smaller, 0.165 vs 0.67 eV (at 290 K). The contribution to resolution (in MeV) due to the statistics of charge collection is given by

$$\Delta E_F = 2.355\ (F\varepsilon E_\gamma)^{1/2} \quad ,$$

where F is the Fano factor, ε is the average energy (in eV) needed to form an electron-hole pair, and E_γ is the γ-ray energy (in eV). Assuming ε to scale with the band gap and the Fano factor to be comparable to that for Ge, this yields a resolution for InSb better than that of Ge by a factor of at least two. Folding this in, we obtain a peak-to-Compton ratio improved by a factor of at least 12.

Unfortunately, difficulties immediately arise. The electron mobility is higher than the hole mobility by a factor of 100. This leads to three separate, but related, problems.

First, the problem of compensation. In the early days of Ge detector fabrication, when "intinsically pure" Ge was not available, it was possible to compensate p-type Ge by drifting it with Li^+ ions. Drifting InSb, however, is out of the question: The difference between the electron and hole mobilities in InSb means that

Li^+ drifting of p-type InSb is impossible; indeed, p-type InSb itself is not readily produced. Instead, drifting n-type InSb with a small anion would be necessary, and F^-, the smallest anion, is many times as large as Li^+. And the small InSb band gap makes drifting at elevated temperatures unfeasible, so drifting becomes impossibly slow. The solution to this first problem is to be able to fabricate detectors from "intrinsic quality" InSb. Zone-refining techniques have now developed to the point that such quality InSb is becoming commercially available, at least for very small infra-red detectors.

The second, problem is that of complete charge collection. The relatively slow hole mobility is a potential source of trouble. Energy resolutions approaching those of the best Ge detectors will require a ratio of collected charge to total deposited charge approaching 98 percent or better. It should be noted that there are also stoichiometric problems associated with growing extremely pure crystals of mixed semiconductors that are not encountered in growing extremely pure crystals of Si or Ge.

Third, the problem of geometry on charge collection and resolution. Trapping and incomplete charge collection would not be such a problem if it were possible to guarantee uniformly incomplete charge collection. Unfortunately, this approaches becoming possible only for very small detectors. As a result, detectors fabricated out of materials having widely different electron and hole mobilities show a decided geometrical dependence on the degree of (hole) trapping and thus a dependence on where in the detector the γ-ray interaction took place. Interactions taking place near the negative contact, in which the electrons traverse the entire width of the detector, show much more complete charge collection than do interactions taking place near the positive contact.

Luckily, the very cause of the difficulty, i.e., the differences in mobility, also furnishes a solution to this third problem. There is a similar geometrical dependence on pulse rise-time, with pulses having more complete charge collection being faster than those having less complete charge collection. Two types of electronic pulse-height correction have been developed to compensate for this. The first was developed to compensate for this problem in HgI_2 detectors.[4] The second was developed in our laboratory to compensate for varying incomplete charge collection in neutron-damaged Ge detectors[3]; it can also compensate for geometrical effects on rise-time in coaxial detectors. Both methods are equally applicable to solving this problem with InSb, requiring only slightly more complex electronics than are normally used for self-gated-singles coincidence experiments.

On paper InSb shows great potential for fabricating superior γ-ray detectors. However, it is decidedly not an easy material to deal with, and we have covered some of its pitfalls. What about practical γ-ray detectors?

InSb cannot be drifted for compensation, but it shows promise for becoming available in quality good enough for "intrinsic" detectors, requiring no compensation. It has no destructive solid-state phase transitions (as contrasted with materials such as HgI_2), and zone-refining techniques have reached the point that very small "intrinsic" detectors are now commercially available for infra-red spectroscopy. The promise of InSb is great enough that working out techniques for dealing with it should definitely be worth the effort. We are currently in the process of converting and testing several of these detectors for γ-ray spectroscopy. Results should be forthcoming in the near future.

References

1. P. J. Twin, P. J. Nolan, R. Aryaeinejad, D. J. G. Love, A. H. Nelson, and A. Kirwan, Nucl. Phys. A409 (1983) 343c.
2. The following are more or less typical of the numerous proposals of recent years: "The High Resolution Ball", R. M. Diamond and F. S. Stephens, Lawrence Berkeley Laboratory, 1981; "Proposal for a MultiElement High Resolution Anti-Compton Shielded Detector Array with a Total Energy Multiplicity Spectrometer", J. X. Saladin et al., Univ. of Pittsburgh, 1982.
3. M. Matsushita, Wm. C. McHarris, R. B. Firestone, J. Kasagi, and W. H. Kelly, Nucl. Instr. and Meth. 179 (1981) 119; N. Matsushita, J. Kasagi, and Wm. C. McHarris, Nucl. Instr. and Meth. 201 (1982) 433.
4. M. Finger, T. A. Prince, L. Padgett, B. Prickett, and W. Schnepple, IEEE Trans. Nucl. Sci. NS-31 (1984) 348.
5. R. C. Whited and M. M. Schieber, Nucl. Instr. and Meth. 162 (1979) 113.

SPURIOUS FLUCTUATIONS IN SPECTRA FROM POSITION DETECTORS CAUSED BY THE DIVISION OF SMALL INTEGERS.

J.S. Winfield and W.N. Catford[a]

A common technique for obtaining a position parameter from e.g. a resistive wire counter, is to divide the voltages from charge-sensitive preamplifiers connected to either end of the counter.[1] The division operation may be performed by an analog divider, or to avoid possible non-linearities, by the data analysis software. In the latter case, the signals from the ends of the counter are digitally encoded before transmission to the software. This is generally a satisfactory technique, but it does have a potential problem associated with the division of small integers. Unless the digitized signals are greater than a certain size (estimated below), a significant amount of accuracy is lost and spurious fluctuations may occur in the position spectrum.

Consider a division operation of the form

$$P = \frac{A}{C} \times \frac{L}{L + R}$$

where L and R are the integer results of digital conversion of the signals, A is the number of channels in the ADC and C is the compression factor used in the generation of the histogram (i.e. the number of bins in the histogram is A/C). If the values of L and R are small relative to A/C (due to low amplifier gains or because the detected particles are lowly-ionizing) certain values of P will be suppressed and other values enhanced. For example, if A=512, C=1, and L≤R≤125, a result of P=255 cannot be obtained whereas P=256 can be made from many combinations of L and R. This effect produces sharp oscillations in the histogram, particularly at $\frac{1}{2}$, $\frac{1}{3}$, and $\frac{2}{3}$ of the spectrum length (Fig. 1).

By consideration of a range of L values for a given R near the central region of the counter (i.e. L≈R), we find that the requirement for all values of P to be obtainable is that L≥(A/2C). This criterion agrees with empirical findings from Monte Carlo simulations with several overall L and R gains. To avoid the specification "near the center of the counter", the criterion may be expressed as (L+R)≥(A/C).

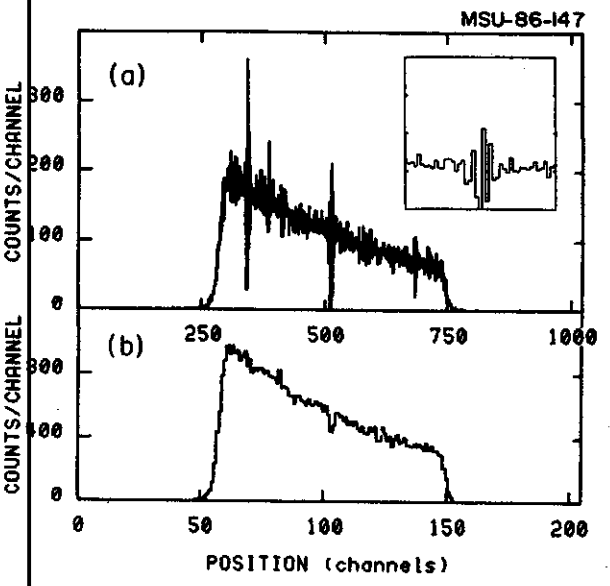

Fig. 1 (a) Histogram of position of α-particles detected by a proportional counter at the focal plane of the S-320 spectrograph. Because the gains of the counter and amplifiers were set for the detection of ^{12}N ions, the signals for the α-particles were only about 1/40th of the ADC full scale. The histogram is compressed by a factor of four. The insert shows a detail of the central region. (b) The same histogram compressed by an additional factor of five. This almost satisfies the condition (L+R)≥(A/C). The oscillations have virtually disappeared.

If the gains of L and R cannot be raised for some reason, the effect of the division of small integers may be alleviated by compressing the histogram (summation of neighboring bins). The consequent loss of resolution could be avoided by the use an ADC with more channels.

---

a. Australian National Univ., Canberra.

Reference

1. See, e.g., J.L.C. Ford, Nucl. Instrum. Methods 162,277(1979).